1　*Revision 1*

2

3　**The relation between Li ↔ Na substitution and hydrogen bonding in five-periodic**

4　**single-chain silicates nambulite and marsturite: A single crystal X-ray study**

5

6　Mariko Nagashima[1],　Thomas Armbruster[2], Uwe Kolitsch[3,4] and Thomas Pettke[5]

7

8　[1] Graduate School of Science and Engineering, Yamaguchi University, Yamaguchi

9　753-8512, Japan

10　[2] Mineralogical Crystallography, Institute of Geological Sciences, University of Bern,

11　Freiestrasse 3, CH-3012 Bern, Switzerland

12　[3] Mineralogisch-Petrographische Abt., Naturhistorisches Museum, Burgring 7, A-1010

13　Wien, Austria

14　[4] Institut für Mineralogie und Kristallographie, Universität Wien, Geozentrum, Althanstr.

15　14, A-1090 Wien, Austria

16　[5] Institute of Geological Sciences, University of Bern, Baltzerstrasse 1+3, CH-3012

17　Bern, Switzerland

18

19　E-mail: nagashim@yamaguchi-u.ac.jp (corresponding author),

20　thomas.armbruster@krist.unibe.ch

21

22　Running title: Crystal chemistry of nambulite and marsturite

23　*Message to Associate editor and reviewers*: Tables 2, 4, and 5 were prepared as

24　deposited items. Thank you.

ABSTRACT

Isomorphic nambulite, natronambulite, marsturite and lithiomarsturite belong to the p-p (pectolite-pyroxene) series of pyroxenoid group minerals with five-periodic single chains of tetrahedra and the common simplified composition (Li, Na)(Mn,Ca)$_4$[Si$_5$O$_{14}$(OH)] ($Z = 2$, space group $P\bar{1}$). New crystal structure refinements including localization of H positions of four samples (two nambulite, one natronambulite, and one marsturite) with varying Li and Na concentrations and major to trace element compositional data from different localities are presented. Na occupies a strongly distorted eight-fold coordinated site (M5). Lithium replacing Na has a substantially smaller ionic radius and occupies a pocket of the large M5 coordination polyhedron and is only five-fold coordinated by oxygen. Thus, the Li $\leftrightarrow$ Na substitution has a significant influence on the bond-valence sums of oxygen sites forming the large cage around M5. Two of the cage-building oxygen sites (O1 and O11) are involved in hydrogen bonding. If M5 is occupied by Na or empty as in the closely related babingtonite, Ca$_2$Fe$_2$[Si$_5$O$_{14}$(OH)], the OH-group is at O1 and exhibits a strong hydrogen bond to O11. If a pocket of M5 is occupied by Li, the hydrogen bond system is reversed with OH at O11 and a strong hydrogen bond to O1. This study emphasizes that short hydrogen bonds with O-H$^{..}$O separations of ca. 2.46 Å may be modified by homovalent substitution, which contributes to the understanding of strong hydrogen bonds and their role in the stability of hydrous pyroxenoids with strongly curled silicate chains.

Keywords: nambulite, marsturite, pyroxenoid, Fianel, Molinello, Gozaisho, crystal structure, hydrogen-bonding

INTRODUCTION

Nambulite, (Li,Na)Mn$_4$[Si$_5$O$_{14}$(OH)], natronambulite, (Na,Li)Mn$_4$[Si$_5$O$_{14}$(OH)], lithiomarsturite, (Li,Na)Ca$_2$Mn$_2$[Si$_5$O$_{14}$(OH)], and marsturite, (Na,Li)CaMn$_3$[Si$_5$O$_{14}$(OH)], belong to the p-p (pectolite-pyroxene) series of pyroxenoid-group minerals with five-periodic single chains. Their triclinic crystal structures ($Z = 2$) are isomorphic.

Nambulite from the Funakozawa mine, Iwate, Japan was first defined as a new species by Yoshii et al. (1972) although a corresponding mineral had already been described as a Li-containing hydrous manganese metasilicate from a high grade regional metamorphic rock in India (Ito 1972). Narita et al. (1975) solved the crystal structure of nambulite from the Funakozawa mine and emphasized its close relation to that of babingtonite. Li-hydropyroxenoids were synthesized by Ito (1972). The end member LiMn$_4$Si$_5$O$_{14}$(OH) (referred to as Li-hydrorhodonite in his paper) formed over a wide P-T field ranging from 500°C at 300 MPa up to 750 °C at 200 MPa. He concluded that the maximum sodium substitution on the join LiMn$_4$Si$_5$O$_{14}$(OH)-NaMn$_4$Si$_5$O$_{14}$(OH) does not exceed Li$_{0.7}$Na$_{0.3}$ under his experimental conditions (most of the runs were within the range of 500 °C/300 MPa and 850 °C/150 MPa).

The Na-analogue of nambulite, natronambulite, was discovered as an independent mineral from the Tanohata mine, Iwate, Japan (Matsubara et al. 1985). Mukhopadhyay et al. (2005) suggest that low pressure conditions stabilize Na-rich nambulite rather than Li-rich compositions. However, they also mention that the local bulk chemistry is crucial.

The occurrence of nambulite is uncommon. In addition to the localities mentioned above, it has been reported from the Kombat mine, Namibia (von Knorring

73 et al. 1978; Dunn 1991), from the Cerchiara mine, Italy (Balestra et al. 2009), and from

74 manganiferous metatuffs of the Ossa-Morena Central Belt in SW Spain (Velilla and

75 Jiménez-Millán 2012). Recently, nambulite was discovered from the Fianel Fe-Mn mine,

76 Val Ferrera, Graubünden, Switzerland (Nagashima and Armbruster 2012).

77   Marsturite was first described by Peacor et al. (1978) from Franklin, New

78 Jersey, USA. At this locality, marsturite is associated with rhodonite, willemite, and

79 abundant axinite-(Mn). Lithiomarsturite from the Foote pegmatite mine (North Carolina,

80 USA) was later defined by Peacor et al. (1990) as the Li-dominant analogue of

81 marsturite. Interestingly, the Mn/Ca ratio of lithiomarsturite is approximately 1 whereas

82 marsturite has a corresponding ratio of 3. Kolitsch (2008) presented, in a conference

83 abstract, the crystal structure of marsturite from the Molinello mine, Liguria, Italy,

84 details of which are summarized in this paper, along with new electron microprobe data.

85 The crystal structure of lithiomarsturite from the type locality (Foote mine, North

86 Carolina) was recently reported (Yang et al. 2011).

87   The structure of the aforementioned isomorphic minerals contains an

88 undulating chain built by five SiO_4 tetrahedra per repeat unit (*fünfereinfach-chain* of

89 Liebau 1985), three crystallographically independent octahedra, M1-M3, and

90 seven-coordinated M4. The M1-M4 sites are mainly occupied by Mn^{2+} in nambulite. In

91 marsturite, the M1-M3 sites are predominantly occupied by Mn^{2+} but M4 hosts Ca. In

92 the case of lithiomarsturite, Ca ions additionally occupy M2. Li and Na are located at

93 M5. The structural study of Indian nambulite (Murakami et al. 1977) revealed that Mg

94 is preferentially located at a specific position (M3) and the high Li content deforms the

95 $M5O_8$ polyhedra to distorted octahedra. The decrease of the coordination number of M5

96 due to increased Li content is also supported by the structural study of lithiomarsturite

4

97   (Yang et al. 2011). Thus, the coordination number of M5 varies from six to eight

98   depending on the dominant alkali cation.

99   In this study, we investigated the crystal chemistry of two nambulite, one

100 natronambulite, and one marsturite crystals in order to examine structural and

101 compositional variations. The following experimental methods were used:

102 electron-microprobe analysis (EMPA), laser-ablation inductively coupled-plasma mass

103 spectrometry (LA-ICP-MS), and single-crystal X-ray diffraction methods. A

104 bond-valence analysis was also carried out.

105

106   **EXPERIMENTAL METHODS**

107 **Samples**

108 Nambulite: (1) A specimen from the manganese ore deposit of the Fianel mine

109 in Val Ferrera, Graubünden, Switzerland (Nagashima and Armbruster 2012) was studied.

110 Nambulite occurs as small, anhedral, transparent yellow crystals (less than 500 µm)

111 embedded in a quartz-palenzonaite matrix (Fig. 1). The nambulite crystal contains

112 enclosed rhodonite. The hand specimen used for this study was identical to that used for

113 the palenzonaite study by Nagashima and Armbruster (2012). (2) A specimen from the

114 metamorphosed manganese ore deposit of the Gozaisho mine in Iwaki, Fukushima,

115 Japan (Matsubara 1977; Matsubara et al. 1996) was analyzed. The area of the deposit

116 underwent amphibolite-epidote facies metamorphism. At this locality, nambulite occurs

117 as anhedral, transparent yellowish orange crystals up to ca. 1 mm scattered within a

118 quartz-braunite matrix.

119 Natronambulite: The investigated specimen also originated from the Gozaisho

120 mine. The occurrence of natronambulite is very similar to that of nambulite from this

121 locality. Pale yellow, transparent natronambulite crystals are embedded in black

122 manganese ore mainly composed of braunite and quartz. The anhedral natronambulite

123 crystals tend to be larger than our nambulite crystals and are up to *ca*. 3 mm.

124   Marsturite: Two visually similar specimens from the Molinello mine, a

125 metamorphosed manganese ore deposits in Val Graveglia, Liguria, Italy, were studied.

126 In both samples, marsturite occurs as pale orange-brown indistinct prismatic crystals in

127 calcite veinlets. Only one sample was studied by single-crystal X-ray diffraction. The

128 studied crystal fragment is identical to that reported by Kolitsch (2008).

129

130 **Chemical analysis**

131 *Electron microprobe analyses*

132 The chemical compositions of nambulite, natronambulite and marsturite were

133 determined using a JEOL JXA-8230 electron microprobe analyzer (EMPA) at

134 Yamaguchi University. Operating conditions were: accelerating voltage of 15 kV, a

135 beam current of 20 nA, and a beam diameter of 1-10 μm. Wavelength-dispersion spectra

136 were collected with LiF, PET, and TAP monochromator crystals to identify interfering

137 elements and locate the best wavelengths for background measurements. The

138 abundances of Si, Ti, Al, Cr, V, Fe, Mn, Ni, Mg, Ca, Sr, Ba, Na, K, As, P, Pb, Zn, F, and

139 Cl were measured. Several elements were below the respective detection limits and thus

140 not shown in Table 1. The following standards were used: wollastonite (Si, Ca), rutile

141 (Ti), corundum (Al), eskolaite (Cr), $Ca_3(VO_4)_2$ (V), hematite (Fe), manganosite (Mn),

142 NiO (Ni), periclase (Mg), $SrBaNb_4O_{12}$ (Sr, Ba), albite (Na), K-feldspar (K), GaAs (As),

143 $KTiOPO_4$ (P), cerussite (Pb), ZnO (Zn), fluorite (F), and halite (Cl). The ZAF

144 correction-method was used for all elements. The cation ratio was normalized on the

145 basis of Si + V^{5+} + As^{5+} = 5. The Li concentration of natronambulite and marsturite was

146 calculated based on charge balance.

147

148 *Laser-ablation inductively coupled-plasma mass spectrometry (LA- ICP-MS)*

149 The Li_2O concentration of two nambulite specimens was confirmed by laser ablation

150 inductively coupled-plasma mass spectroscopy (LA-ICP-MS) installed at University of

151 Bern. The instrument consists of a pulsed 193 nm ArF Excimer laser (Lambda Physik,

152 Germany) with an energy-homogenized Geolas Pro optical system (Microlas,

153 Germany), coupled with an ELAN DRC–e ICP quadrupole mass spectrometer (Perkin

154 Elmer, USA) operated in standard mode. The instrument was tuned to robust plasma

155 conditions. A spot size between 18 and 44 μm was used, and the counting time was > 50

156 seconds for the background and up to 50 seconds for sample analysis (beam size

157 permitting). The instrument was calibrated against NIST SRM 610 glass. Data reduction

158 employed the program SILLS (Guillong et al. 2008), with internal standardization using

159 EMPA SiO_2 concentration data. More details about instrumental operating conditions

160 and calculation of the limits of detection can be found in Pettke et al. (2012).

161

162 *Single-crystal X-ray structural analysis*

163 X-ray diffraction data for single-crystals of nambulite and natronambulite were

164 collected using a Bruker SMART APEX II CCD diffractometer installed at University

165 of Bern. Crystals were mounted on glass fibers and intensity data were measured at

166 room temperature using graphite-monochromatized Mo$K\alpha$ radiation (λ = 0.71069 Å).

167 Preliminary lattice parameters and an orientation matrix were obtained from three sets

168   of frames and refined during the integration process of the intensity data. Diffraction

169   data were collected with ω scans at different φ settings (φ-ω scan) (Bruker 1999). Data

170   were processed using SAINT (Bruker 1999). An empirical absorption correction using

171   SADABS (Sheldrick 1996) was applied. X-ray diffraction data for a crystal fragment of

172   marsturite, mounted on a glass fiber, was collected at room temperature using a Nonius

173   KappaCCD diffractometer at the University of Vienna and φ-ω scans (Mo$K\alpha$ radiation,

174    $\lambda = 0.71069$ Å). The measured intensity was processed with the Nonius program suite

175   DENZO-SMN and corrected for Lorentz, polarization, background, and, using the

176   multi-scan method (Otwinowski et al. 2003) absorption effects. As reported by Narita et

177   al. (1975), $P\bar{1}$ was found to be the correct space group for all nambulite samples.

178   Crystal structure refinements were performed using SHELXL-97 (Sheldrick 2008).

179   Scattering factors for neutral atoms were employed throughout.

180   In case of nambulite and natronambulite, although the site occupancies of

181   M1-M4 were refined with Mn without restraints in preliminary refinements, those of

182   M1 and M2 turned out to be 1.0 Mn within standard deviation. Thus, the occupancies at

183   these two sites were fixed as 1.0 Mn atoms per formula unit (apfu) in the final

184   refinements. Those at M3 and M4 were refined with Mn to derive the site-scattering

185   values for the determination of site populations. In case of marsturite, the site

186   occupancies were refined with Mn for M1-M3 and Ca for M4 without restraints in a

187   preliminary refinement. The occupancy of M1 turned out to be 1.0 Mn within standard

188   deviation and was correspondingly fixed. Occupancies of M2 and M3 were below 1 and

189   that of M4 above 1. Based on the chemical formula, volume of polyhedra, and the

190   studies on marsturite (Peacor et al. 1987) and lithiomarsturite (Murakami et al. 1977;

191   Yang et al. 2011), occupancies in final cycles were refined with Mn and Ca at M2 and

8

192 M4, and with Mn and Mg at M3. In both minerals, the site occupancy of M5 was

193 refined with Na and Li scattering factors. Although closely-spaced individual positions

194 of Na and Li were resolved in natronambulite, their anisotropic displacement parameters

195 were restrained to be equal. The occupancies at Si1-Si5 were fixed as 1.0 Si apfu.

196 Position of the hydrogen atoms of the hydroxyl groups in Gozaisho nambulite,

197 natronambulite, and marsturite were derived from difference-Fourier synthesis.

198 Subsequently, hydrogen positions were refined at a fixed value of U_{iso} = 0.05 Å^2 and a

199 bond distance restraint of O–H = 0.980(1) Å (Franks 1973). In natronambulite, two H

200 atom positions were refined. The occupancies of H1 and H11 were fixed as 30% and

201 70%, respectively, according to corresponding Li and Na occupancies (see discussion

202 section).

203

204   **RESULTS**

205 **Chemical compositions of nambulite**

206 The average chemical compositions of the studied nambulite, natronambulite, and

207 marsturite samples are given in Table 1. As mentioned, the Li_2O concentrations of the

208 two nambulite samples were obtained by LA-ICP-MS. The Li_2O concentrations in the

209 others were estimated by charge balance. These estimated values are in good agreement

210 with the Li concentrations derived from the structural analysis.

211   The Gozaisho nambulite crystals are relatively homogeneous. Crystals of

212 Fianel nambulite exhibited rhodonite inclusions (Fig. 2). The natronambulite crystals

213 are homogeneous but albite (Ab_{100}) inclusions were rarely observed. The Molinello

214 marsturite contained only negligible inclusions. The crystals used for structural analysis

215 were picked from the same hand specimens. The nambulite crystal from Fianel

9

216 measured by X-ray diffraction was a single phase as evaluated with a polarizing

217 microscope.

218   Trace element concentrations range from 0.01 to about 2000 μg g^{-1} (Table 2).

219 They are variable between samples from Fianel and Gozaisho as portrayed in Fig. 3.

220 Fianel nambulite contains much more V and Zn, variably more B, Sr, Ba, As and Pb.

221 Primitive mantle normalized rare earth element (REE) patterns are heavy REE enriched,

222 for nambulite from Gozaisho more so than that from Fianel. Gozaisho nambulite

223 contains markedly higher concentrations of Co and Cu and elevated Sc.

224

225 **Crystal-structure solution and refinements**

226   Crystallographic data and refinement parameters are summarized in Table 3.

227 Structure refinements in this study converged to R_1 values of 1.56-5.53%. The refined

228 atomic positions and anisotropic mean square displacement parameters are listed in

229 Tables 4 and 5. The Na and Li positions at M5 in natronambulite are separately shown

230 in Table 4. The site-scattering values are shown in Table 6. Interatomic distances are

231 presented in Table 7. The crystal structure of nambulite, which is isomorphic with

232 marsturite, is shown in Fig. 4.

233

234   **DISCUSSION**

235 **Cation distribution and structural variations**

236 In this study, cation distributions at the octahedral M1-M3 and seven-coordinated M4

237 sites in nambulite were determined from the chemical compositions, refined site

238 scattering values, volumes of coordination polyhedral, and bond distances. Consistent

239 with the mean bond distances (Table 7) of M1-O (ca. 2.22 Å) and M2-O (ca. 2.22-2.23

10

240   Å) M1 and M2 are occupied by only Mn (No. e^- = 25). A low site-scattering value (< 25

241   e^-) at M3 and the mean M3-O distance of ca. 2.17 Å suggest Mn and Mg at M3. The

242   low site-scattering value (< 25 e^-) at M4 associated with the mean M4-O distance of ca.

243   2.4 Å indicates Mn and Ca at M4 (Table 6). The number of electrons obtained from the

244   refined site occupancies is consistent with the ones calculated from EMA results. Mg at

245   M3 was also reported for Indian nambulite by Murakami et al. (1977). In case of

246   marsturite, Ca predominantly occupies the seven-coordinated M4 site ($Ca_{0.76}Mn_{0.24}$). As

247   the result of structural analysis, M1 is fully occupied by Mn, however, the observed

248   site-scattering values of M2 and M3 were below 25. Both M2 and M3 are

249   predominantly occupied by Mn, but small amounts of Ca, Mg, and Fe are also present

250   based on the chemical composition. The <M2-O> and <M3-O> distances of marsturite

251   are 2.251 and 2.187 Å, respectively (Table 7). In comparison with <M1-O> (= 2.222 Å),

252   <M2-O> is longer and <M3-O> is shorter. This indicates that a cation having a larger

253   ionic radius than that of Mn^{2+} (0.83 $Å^{VI}$ in Shannon 1976) occupies M2 and the smaller

254   cation M3. Therefore, Ca (1.00 $Å^{VI}$) prefers M2 whereas Fe (0.78 $Å^{VI}$) and Mg (0.72

255    $Å^{VI}$) prefer M3 in marsturite. The M5 site is occupied by Li and Na. According to the

256   refinements, the site occupancy of M5 is $Li_{0.72}Na_{0.28}$ in Fianel nambulite and $Li_{0.82}Na_{0.18}$

257   in the Gozaisho one. The site occupancy of M5 in natronambulite is $Na_{0.72}Li_{0.28}$. The

258   M5 site is mainly occupied by Na ($Na_{0.94}Li_{0.06}$) in marsturite, in very good agreement

259   with the EMPA data.

260   Unit-cell parameters of nambulite from both localities are similar (Table 3).

261   They are close to those reported by Murakami et al. (1977), but smaller than those

262   reported by Narita et al. (1975). The lengths of the **a**- and **c**-axes of natronambulite

263   almost correspond to those from the Tanohata mine, Japan, reported by Matsubara et al.

264   (1985), but the **b**-axis length determined here is shorter than for their natronambulite

265   [11.7340(2) Å in this study; 11.762 Å in Matsubara et al. (1985)]. The unit-cell volume

266   of natronambulite is larger than that of nambulite due to the high Na content. The ionic

267   radii of Na and Li in eight-fold coordination are 1.18 and 0.92 Å (Shannon 1976),

268   respectively. Due to the higher Ca content of marsturite, its unit-cell volume is larger

269   than those of nambulite and natronambulite. Comparing marsturite and lithiomarsturite,

270   the unit-cell volume of marsturite is smaller than that of lithiomarsturite. Although

271   lithiomarsturite is poor in Na and rich in Li, the Ca:Mn ratio in lithiomarsturite is 2:2

272   instead of 1:3 in marsturite. Thus, the large ionic radius of Ca^{2+} and its high amount are

273   responsible for the large cell volume.

274   In the two investigated nambulite samples, the high Li content at M5 modifies

275   the arrangement of O atoms defining the M5 polyhedra. The M5 polyhedra of the

276   Na-dominant species, such as natronambulite and marsturite, have eight-fold

277   coordination by O1, O3, O6, O11, O14, O15 and O15' in Fig. 4b. The increase in Li

278   content reduces the eight-fold coordination of M5 to a distorted six-coordinated site as

279   Murakami et al. (1977) pointed out. However, the new data (Table 7) strongly suggest

280   that five-fold coordination by O1, O3, O11, O14 and O15 (Fig. 4b) is a more reasonable

281   description for Li-rich M5. With increasing Li content, the ligands O14, O3, O1 and

282   O15 (1st to 4th neighbor oxygens in case of Gozaisho nambulite) are getting closer to the

283   cation at M5 whereas the distances from M5 to O6 (7th neighbor) and O12 (8th

284   neighbor) increase. With increase of Li content, the cation at M5 shifts toward the

285   Si1O$_4$-tetrahedron [Si1-M5 distance = 3.043 Å in the Gozaisho sample, and 3.176 Å in

286   the Funakozawa sample by Narita et al. (1975)] and away from Si4O$_4$ [Si4-M5 distance

287   = 3.290 Å in the Gozaisho sample, and 3.144 Å in the Funakozawa sample by Narita et

12

288   al. (1975)] (Fig. 5).

289   The periodicity of the *fünfereinfach-chain* (Fig. 4) in nambulite spans 12.05 Å

290   (this study), in natronambulite 12.02 Å (this study), in lithiomarsturite 12.12 Å (Yang et

291   al. 2011), in marsturite 12.02 Å (this study), and in babingtonite

292   ($Ca_2Fe^{3+}Fe^{2+}[Si_5O_{14}(OH)]$) 12.17 Å (Nagashima et al. 2013). The chain curls on an

293   underlay formed by M1-M4 polyhedra filled by cations with varying mean ionic radius:

294   Nambulite and natronambulite 0.83 Å, lithiomarsturite 0.92 Å, marsturite 0.87 Å, and

295   babingtonite 0.85 Å after ionic radii of Shannon (1976). Thus, the repeat length of the

296   chain of tetrahedra is not directly linked to the average cation size at M1-M4. The

297   Si1-O3-Si2 angle (Table 8) of Li-dominant specimens (138.1-138.5° in this study) is

298   smaller than in Na-dominant ones (142.5-142.9°). Decrease of the M5-O3 distance with

299   increasing Li at M5 is a main reason of the smaller Si1-O3-Si2 angle. In babingtonite

300   the Si1-O3-Si2 unit bridges corners of the $M2O_6$ octahedron corresponding to M3 in

301   nambulite, which is centered by Fe^{3+} with an ionic radius of only 0.645 Å (Shannon

302   1976). Thus, the Si1-O3-Si2 angle decreases to 136.5° (Nagashima et al. 2013). In

303   nambulite-group minerals, O3 is highly overbonded (2.2-2.4 valence units, vu) whereas

304   in babingtonite, the O6 connecting Si2 and Si3 is highly overbonded [ca. 2.25 vu;

305   Nagashima et al. (2013)]. The short distance of Ca2-O6 (ca. 2.44 Å) in babingtonite,

306   which is topologically similar to M4-O6 (2.5-2.6 Å) in nambulite, is the reason for the

307   over-bonded O6. The Si2-O6-Si3 angle of babingtonite (ca. 144º) is slightly larger than

308   that of nambulite-group minerals (ca. 140º) and probably just compensates the adjacent

309   decreased Si1-O3-Si2 angle.

310

311   **Hydrogen-bonding system in nambulite-group minerals**

13

312   In this study, H positions and the hydrogen bond system were determined for

313   Gozaisho nambulite, natronambulite, and marsturite. One H position is determined in

314   nambulite (H11) and marsturite (H1) structures, though at different oxygen donors. Split

315   H positions were determined in Li-bearing natronambulite (H1 and H11).

316   Based on the results that the M5 site is eight-coordinated for Na-dominant and

317   five-coordinated for Li-dominant species, bond-valence sums were calculated using the

318   electrostatic strength function of Brown and Altermatt (1985) and the bond-valence

319   parameters of Brese and O'Keeffe (1991). The calculated bond-valence sums and

320   refined hydrogen position of Gozaisho nambulite suggest that one hydroxyl group is

321   located at O11 with O1 acting as acceptor (Fig. 5a). The bond-valence sums of O11 and

322   O1 in this nambulite are 1.52-1.55 and 1.76-1.66 vu, respectively (Table 9). The short

323   distance between O1 and O11 has already been predicted as involving a very strong

324   hydrogen bond in members of the pectolite-pyroxenoid series (Murakami et al. 1977).

325   The hydrogen position, however, could not be resolved in their study. Yang et al. (2011)

326   predicted that O11 becomes the hydroxyl group in Li- or Na-containing rhodonite group

327   minerals, such as marsturite, nambulite, and natronambulite. They suggested that the

328   more underbonded O1 (relative to O11) in babingtonite becomes less underbonded in

329   lithiomarsturite. In babingtonite O1 is bonded to two non-hydrogen atoms, Si1 and Ca1,

330   but that in lithiomarsturite it is bonded to Si, Ca, and also to Li (three non-hydrogen

331   atoms). As a consequence, O1-H1 in babingtonite is more tightly bonded than in

332   lithiomarsturite. Thus, O1 is the donor oxygen in babingtonite, but not in

333   lithiomarsturite and nambulite.

334   In contrast with the prediction by Yang et al. (2011), the determined H position

335   (Table 4) and the bond-valence value (Table 9) of marsturite suggest that O1 (1.55 vu)

14

336   acts as a donor oxygen of the hydroxyl group, and O11 (1.65 v.u.) as acceptor oxygen

337   (Fig. 5c). Despite isomorphic structures of nambulite and marsturite, their hydrogen

338   bonding systems are not identical. The hydrogen-bonding system in marsturite is

339   identical to that of babingtonite (Tagai et al. 1990; Nagashima et al. 2013).

340   Li-bearing natronambulite from the Gozaisho mine investigated in this study

341   gives us the clue to understand the hydrogen-bonding system in nambulite and

342   marsturite. Split hydroxyl groups, O1-H1 and O11-H11, are resolved (Fig. 5b). It can be

343   concluded that O1-H1 is associated to Na at M5 and O11-H11 to Li-dominant at M5.

344   This difference is not due to the topology of O1 as Yang et al. (2011) pointed out, but

345   due the different Na and Li positions within the M5 polyhedra. High Li content (= low

346   Na content) leads to strong displacement from the gravity center of the eight-fold

347   coordinated polyhedron around M5 (Table 10 and Fig. 6). High Na content (= low Li

348   content) reduces the out-off center shift. The smaller ionic radius of Li^+ compared to

349   that of Na^+ is the reason that Li prefers a position in a five-coordinated pocket within

350   the large M5 coordination polyhedron. This shift influences the bond-valences of O sites

351   coordinated to M5, such as O1 and O11.

352   M5-O11 of marsturite (2.390 Å) is considerably shorter than that in

353   lithiomarsturite (2.642 Å). The short M5-O11 distance raises the bond-valence of O11.

354   On the other hand, the M5-O1 distance behaves opposite (2.406 Å in marsturite *vs*

355   2.121 Å in lithiomarsturite). Thus, the bond-valence sum of O1 in marsturite is less than

356   that in lithiomarsturite.

357   In summary, we have demonstrated that the very strong hydrogen-bond system in

358   the p-p (pectolite-pyroxene) series of pyroxenoid-group minerals can be reversed by

359   homovalent substitution.

15

360

Trace element patterns of nambulite

Conspicuous variations in some transition metal concentrations of nambulite between Fianel and Gozaisho strongly suggest that trace element patterns of nambulite might be useful for geochemically characterizing their growth environment. For nambulite from Fianel, enrichments in fluid mobile elements B, Sr, Ba, Pb, As and LREE relative to nambulite from Gozaisho suggests the presence of altered source rocks, possibly seawater alteration of the Mesozoic ocean floor materials. The conspicuous relative enrichments in Cu and Co of the Gozaisho nambulite on the other hand may indicate that the source rocks were possibly mineralized in volcanogenic massive sulfide style or hydrothermal activity relating to crystallization of sulfide minerals. Based on the results by Matsubara et al. (1996) on the mineral assemblages of the regionally metamorphosed manganese ore of the Gozaisho mine, nambulite is regarded to have formed by hydrothermal activity with sulfide minerals such as chalcopyrite, galena, molybdenite and pyrite. Thus, the trace element concentration of the Gozaisho nambulite is assumed to be due to rather high metal concentrations in the hydrothermal fluid.

Implications

Ionic, covalent, and hydrogen bonds are the strongest adhesive forces in silicate minerals. Thus, studying the nature of hydrogen bonds is a key discipline in understanding the structure of crystalline solids.

We mainly associate hydrogen bonds with weak bonding interactions like in kaolinite causing hardness between talc and gypsum and clay-like behavior. Hydrogen

16

384   bonds in kaolinite between the layers have a donor-acceptor O-H···O distance of

385   approximately 3 Å and thus allow only weak bonding interactions. The corresponding

386   bond system is composed of a strong O(donor)-H bond of ca. 1 Å and a weak H···O

387   acceptor distance of ca. 2 Å (if straight). However, there are also silicates with strong

388   hydrogen bonds.

389   The chain silicate scheuchzerite (Brugger et al. 2006) exhibits in a topological

390   unit very similar to the minerals investigated in this study (Fig. 5), a donor-acceptor

391   O-H···O distance of only 2.35 Å. Two interpretations were offered (Brugger et al. 2006)

392   either a symmetrical hydrogen bond O···H···O, each with a O-H distance of ca. 1.17 Å or

393   a disordered hydrogen bond with both oxygens occupied in equal proportions by OH.

394   Thus, O-H is ca. 1 Å and H···O is ca. 1.35 Å.

395   Mozartite $CaMn^{3+}O[SiO_3OH]$ and vuagnatite $CaAl(OH)SiO_4$ are isostructural

396   minerals having both a donor-acceptor O-H···O distance of approximately 2.5 Å

397   (Nyfeler et al. 1997). Though, the strong hydrogen-bond system is different. In

398   mozartite OH is part of the SiO_4 tetrahedron (silanol group) with a strong hydrogen

399   bond to an oxygen bonded to two $Mn^{3+}O_6$ octahedra whereas in vuagnatite OH bonds to

400   two AlO_6 octahedra with the acceptor oxygen at the SiO_4 tetrahedron. The reason for the

401   different O-H···O system is an electronic distortion of octahedral $Mn^{3+}O_6$ (Jahn-Teller

402   effect), which shortens the Mn^{3+}-O bonds at the acceptor oxygen and thus increases the

403   bond valence sum. As a consequence the silanol group is formed in mozartite.

404   Serandite and pectolite (Hammer et al. 1998), additional members if the p-p

405   (pectolite-pyroxene) series of pyroxenoid-group minerals with five-periodic single

406   chains, have also short (strong) O-H···O systems in a unit like in Fig. 5 of 2.45 -2.48 Å.

407   In IR spectra these short hydrogen bonds lead to diffuse absorption maxima between

17

408   1300 and 1500 cm^{-1} resembling increased background (Hammer et al. 1998). Thus,

409   strong hydrogen bonds (Libowitzky 1999) may be easily overlooked in IR spectra but

410   are obvious results of crystal-structure refinements accompanied by bond valence

411   calculations.

412   Another crystal-chemical aspect of strong and weak hydrogen bonds should be

413   mentioned. In weak hydrogen bonds $(OH)^-$ may be replaced by F^- or Cl^-. In strong

414   hydrogen bonds this substitution is not favored because short anion-anion distances are

415   strongly repulsive and require shielding. Thus, the proton (H^+) acts as separator between

416   anion charges.

417

425

426   **REFERENCES CITED**

427   Balestra, C., Kolitsch, U., Blass, G., Callegari, A.M., Boiocchi, M., Armellino, G.,

428   Ciriotti, M.E., Ambrino, P., and Bracco, R. (2009) Mineralogia ligure 2007-2008:

429   novità caretterizzate dal Servizio UK dell'AMI. Micro, 1/2009, 78-99 (in Italian).

430   Brese, N.E. and O'Keeffe, M. (1991) Bond-valence parameters for solids. Acta

431   Crystallographica, B47, 192-197.

432   Brown, I.D. and Altermatt, D. (1985) Bond-valence parameters obtained from a

433   systematic analysis of the inorganic crystal structure database. Acta

434   Crystallographica, B41, 244-247.

435   Brugger, J., Krivovichev, S. Meisser, N., Ansermet, S., and Armbruster, T. (2006)

436   Scheuchzerite, $Na(Mn,Mg)_9[VSi_9O_{28}(OH)](OH)_3$, a new single-chain silicate.

437   American Mineralogist, 91, 937–943.

438   Bruker (1999) SMART and SAINT-Plus. Versions 6.01. Bruker AXS Inc., Madison,

439   Wisconsin, USA.

440   Dunn, P.J. (1991) Rare minerals of the Kombat mine Namibia. Mineralogical Record,

441   22, 421-425.

442   Franks, F., Ed. (1973) Water: A comprehensive treatise, vol. 2, 684 pp. Plenum, New

443   York.

444   Guillong, M., Meier, D. L., Allan, M. M., Heinrich, C. A., and Yardley, B. W. D. (2008)

445   SILLS: A MATLAB-based program for the reduction of laser ablation ICP–MS

446   data of homogeneous materials and inclusions. In: Laser ablation ICP-MS in the

447   Earth Sciences: Current practices and outstanding issues (Sylvester, P., ed.).

448   Mineral. Assoc. Can. Short Course Series, 40, 328-333.

449   Hammer, V.M.F., Libowitzky, E., and Rossman, G.R. (1998) Single-crystal IR

450   spectroscopy of very strong hydrogen bonds in pectolite, $NaCa_2[Si_3O_8(OH)]$, and

451   serandite, $NaMn_2[Si_3O_8(OH)]$. American Mineralogist, 83, 569-576.

452   Ito, J. (1972) Synthesis and crystal chemistry of Li-hydro-pyroxenoids. Mineralogical

453   Journal, 7, 45-65.

454   Kolitsch, U. (2008) Implications for the nomenclature of p-p hydropyroxenoids: the

455   crystal structure of marsturite from the Molinello mine, Liguria, Italy. Annual

19

456   Meeting of the DMG, Berlin, Germany, September 14-17, 2008. CD with abstracts,

457   Abs. No. 120.

458   Libowitzky, E. (1999) Correlation of O-H stretching frequencies and O-H···O hydrogen

459   bond lengths in minerals. Monatshefte für Chemie, 130, 1047-1059.

460   Liebau, F. (1985) Structural chemistry of silicates. Springer, Berlin, 347 pp.

461   Matsubara, S. (1977) Nambulite and Li-bearing manganese amphibole from the

462   Gozaisho mine, Fukushima Prefecture, Japan. Annual Meeting of Mineralogical

463   Society of Japan, Abstract A09, page 10 (in Japanese).

464   Matsubara, S., Kato, A., Shimizu, M., Sekiuchi, K., and Suzuki, Y. (1996) Romeite from

465   the Gozaisho mine, Iwaki, Japan. Mineralogical Journal, 18, 155-160.

466   Matsubara, S., Kato, A., and Tiba, T. (1985) Natronambulite, (Na,Li)(Mn,

467   Ca)$_4$Si$_5$O$_{14}$OH, a new mineral from the Tanohata mine, Iwate Prefecture, Japan.

468   Mineralogical Journal, 12, 332-340.

469   Momma, K., and Izumi, F. (2011) VESTA 3 for three-dimensional visualization of

470   crystal, volumetric and morphology data. Journal of Applied Crystallography, 44,

471   1272-1276.

472   Mukhopadhyay, S., Das, K., and Fukuoka, M., (2005) Nambulite,

473   (Li,Na)Mn$_4$Si$_5$O$_{14}$(OH), in the Sausar Group of rocks in Central India. Journal of

474   Mineralogical and Petrological Sciences, 100, 26-30.

475   Murakami, T., Takéuchi, Y., Tagai, T., and Koto, K. (1977) Lithium-hydrorhodonite.

476   Acta Crystallographica, B33, 919-921.

477   Nagashima, M. and Armbruster, T. (2012) Palenzonaite, berzeliite and

478   manganberzeliite: (As^{5+}, V^{5+}, Si^{4+})O$_4$ tetrahedra in garnet structures. Mineralogical

479   Magazine, 76, 1081-1097.

480   Nagashima, M., Mitani, K., and Akasaka, M. (2013) Structural variation of babingtonite

481   depending on cation distribution at the octahedral sites. Mineralogy and Petrology,

482   DOI 10.1007/s00710-013-0297-z

483   Narita, H., Koto, K., Morimoto, N., and Yoshii, M. (1975) The crystal structure of

484   nambulite $(Li, Na)Mn_4Si_5O_{14}(OH)$. Acta Crystallographica, B31, 2422-2426.

485   Nyfeler, D., Hoffmann, C., Armbruster, T., Kunz, M., and Libowitzky, E. (1997)

486   Orthorhombic Jahn-Teller distortion and Si-OH in mozartite, $CaMn^{3+}O[SiO_3OH]$:

487   A single-crystal X-ray, FTIR, and structure modeling study. American

488   Mineralogist, 82, 841-848.

489   Otwinowski, Z., Borek, D., Majewski, W., and Minor, W. (2003) Multiparametric

490   scaling of diffraction intensities. Acta Crystallographica, A59, 228–234.

491   Peacor, D.R., Dunn, P.J., and Sturman, B.D. (1978) Marsturite, $Mn_3CaNaHSi_5O_{15}$, a

492   new mineral of the nambulite group from Franklin, New Jersey. American

493   Mineralogist, 63, 1187-1189.

494   Peacor, D.R., Dunn, P.J.. White, Jr., J.S., Grice, J.D., and Chi, P.H. (1990)

495   Lithiomarsturite, a new member of the pyroxenoid group, from North California.

496   American Mineralogist, 75, 409-414.

497   Pettke, T., Oberli, F., Audetat, A., Guillong, M., Simon, A. C., Hanley, J. J., and Klemm,

498   L. M. (2012) Recent developments in element concentration and isotope ratio

499   analysis of individual fluid inclusions by laser ablation single and multiple collector

500   ICP-MS. Ore Geology Reviews, 44, 10-38.

501   Shannon, R.D. (1976) Revised effective ionic radii and systematic studies of interatomic

502   distances in halides and chalcogenides. Acta Crystallographica, A32, 751–767.

503   Sheldrick, G.M. (1996) *SADABS*. University of Göttingen, Germany.

504   Sheldrick, G.M. (2008) A short history of SHELX. Acta Crystallographica, A64,

505   112–122.

506   Tagai, T., Joswig, W., and Fuess H. (1990) Neutron diffraction study of babingtonite at

507   80 K. Mineralogical Journal, 15, 8-18.

508   Velilla, N. and Jiménez-Millán, J. (2012) Nambulite bearing rock from the Ossa-Morena

509   Central Belt (Iberian Massif, SW Spain). European Mineralogical Conference, Vol.

510   1, EMC2012-385.

511   von Knorring, O., Sahama, T.G., and Törnroos, R. (1978) Second find of nambulite.

512   Neues Jahrbuch für Mineralogie Monatshefte, 1978, H8, 346-348.

513   Yang, H., Downs, R.T., and Yang, Y.W. (2011) Lithiomarturite, $LiCa_2Mn_2Si_5O_{14}(OH)$.

514   Acta Crystallographica E67, i73.

515   Yoshii, M., Aoki, Y., and Maeda, K. (1972) Nambulite, a new lithium- and

516   sodium-bearing manganese silicate from the Funakozawa mine, northeastern Japan.

517   Mineralogical Journal, 7, 29-44.

518

Figure captions

Figure 1 Photograph of a yellow transparent nambulite crystal from the Fianel mine, Switzerland, associated with palenzonaite (dark red) and quartz.

Figure 2 Backscattered electron (BSE) image of the nambulite crystal from the Fianel mine, Switzerland (polished grain mounted in resin). Nam: nambulite, Rdn: rhodonite.

Figure 3 Trace element variation diagram showing individual analyses of nambulite from Fianel normalized to average element concentrations of Gozaisho nambulite.

Figure 4 The arrangement of polyhedra (a) and topological cation environment at M5 (b) of Gozaisho nambulite, iso-morph of marsturite, drawn with VESTA 3 (Momma and Izumi 2011).

Figure 5 Hydrogen-bonding systems with Na and Li positions in nambulite (a), natronambulite (b), and marsturite (c).

Figure 6 The cation shift (Å) from the center of gravity against Li and Na contents at M5 (apfu). The Na and Li positions at M5 in natronambulite were separately determined. Thus, the off-center distance was estimated from individual atomic positions. The shifts derived from Li and Na positions are plotted at 1.0 Li and at 1.0 Na, respectively.

200 μm

Figure 1

Figure 2

Li Na Al Ca Ti Fe Ni Zn Sr Zr Ba Ce Gd Yb W Th
B Mg Si Sc V Co Cu As Y Nb La Nd Er Hf Pb U

Fianel nambulite data points normalized to average Gozaisho nambulite

Figure 3

(a)

(b)

Figure 4

(a) Nambulite

(b) Li-bearing Natronambulite
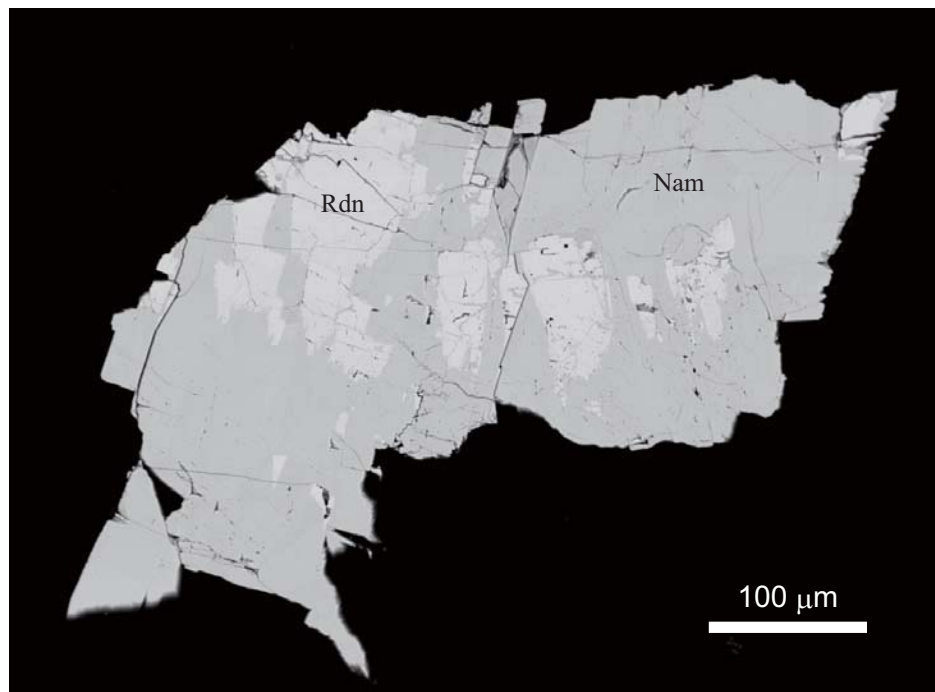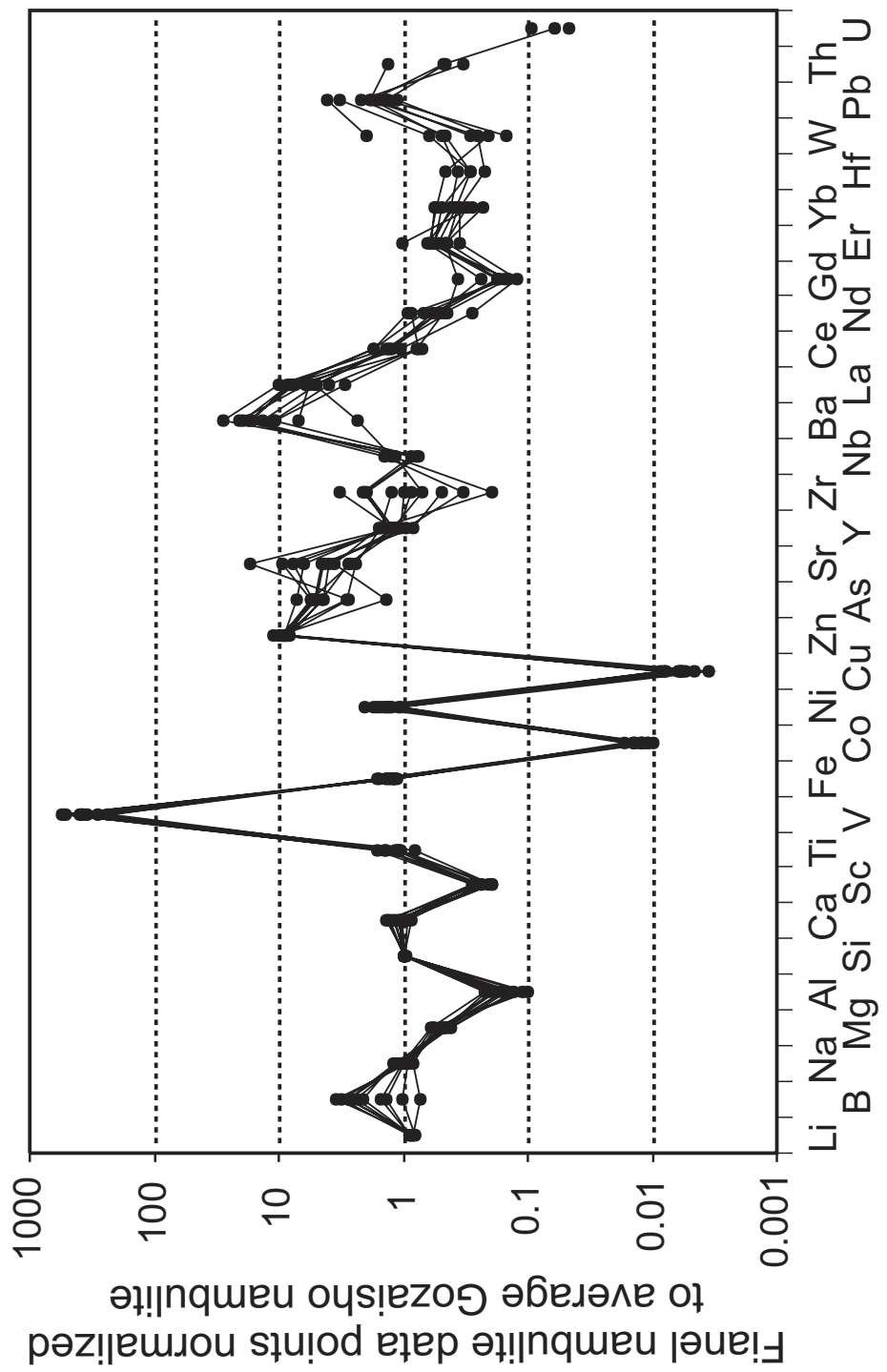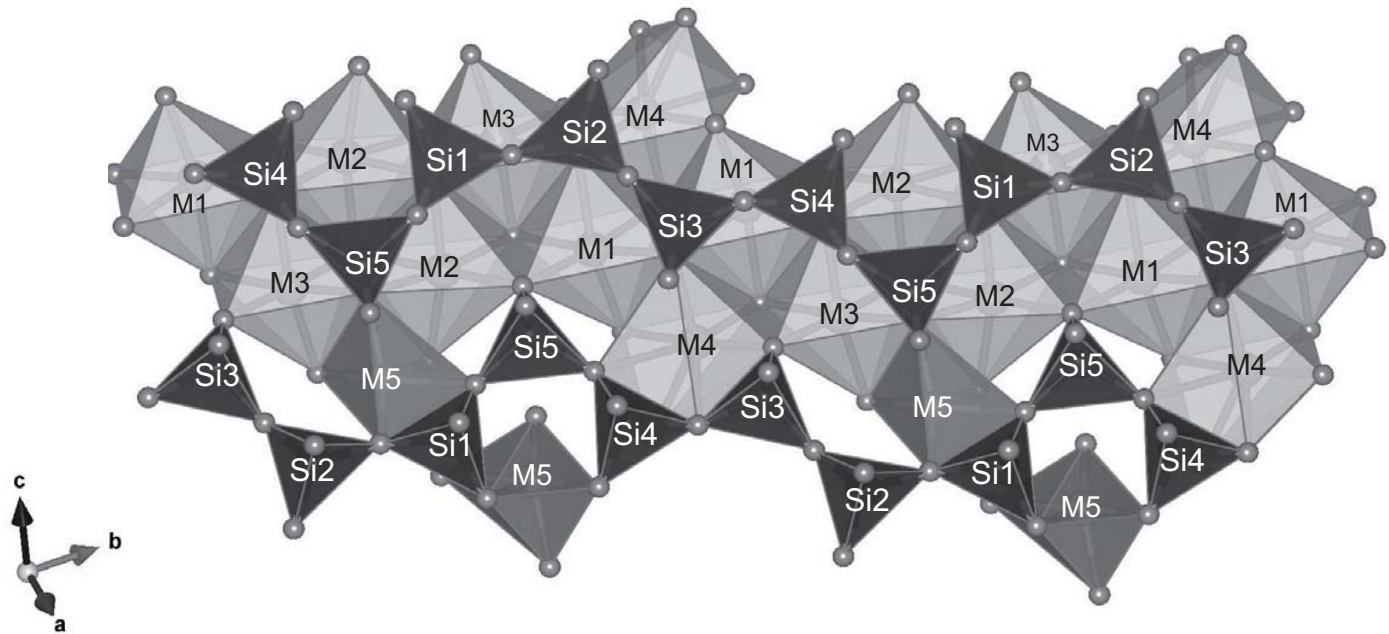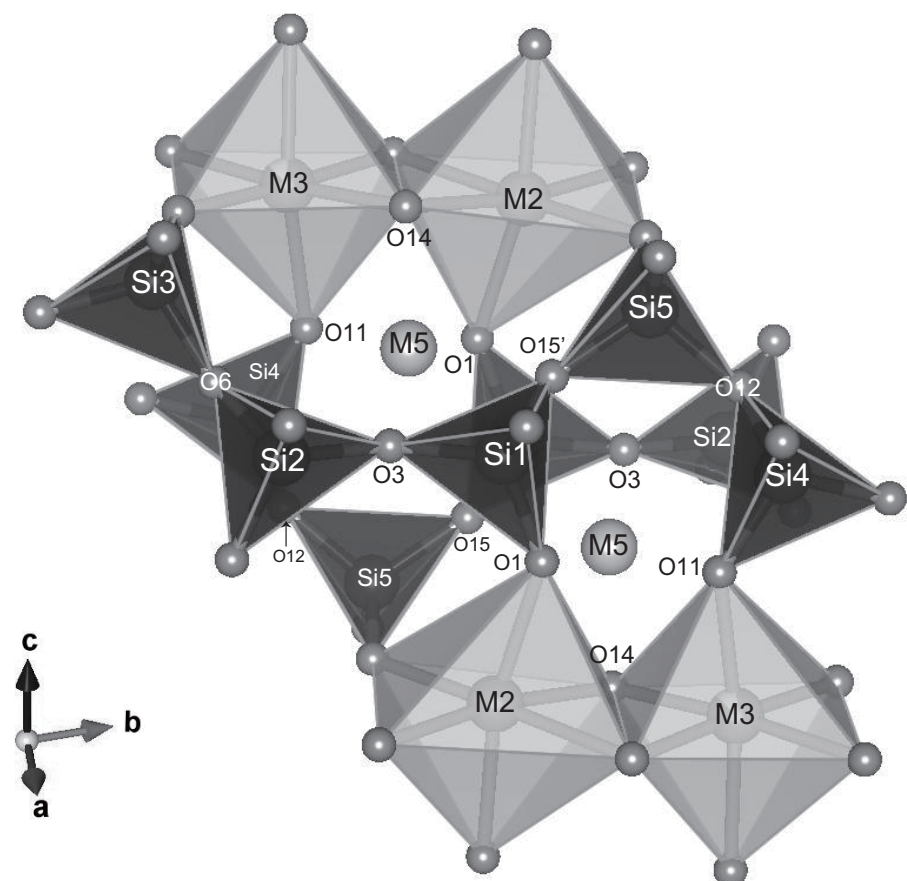
(c) Marsturite
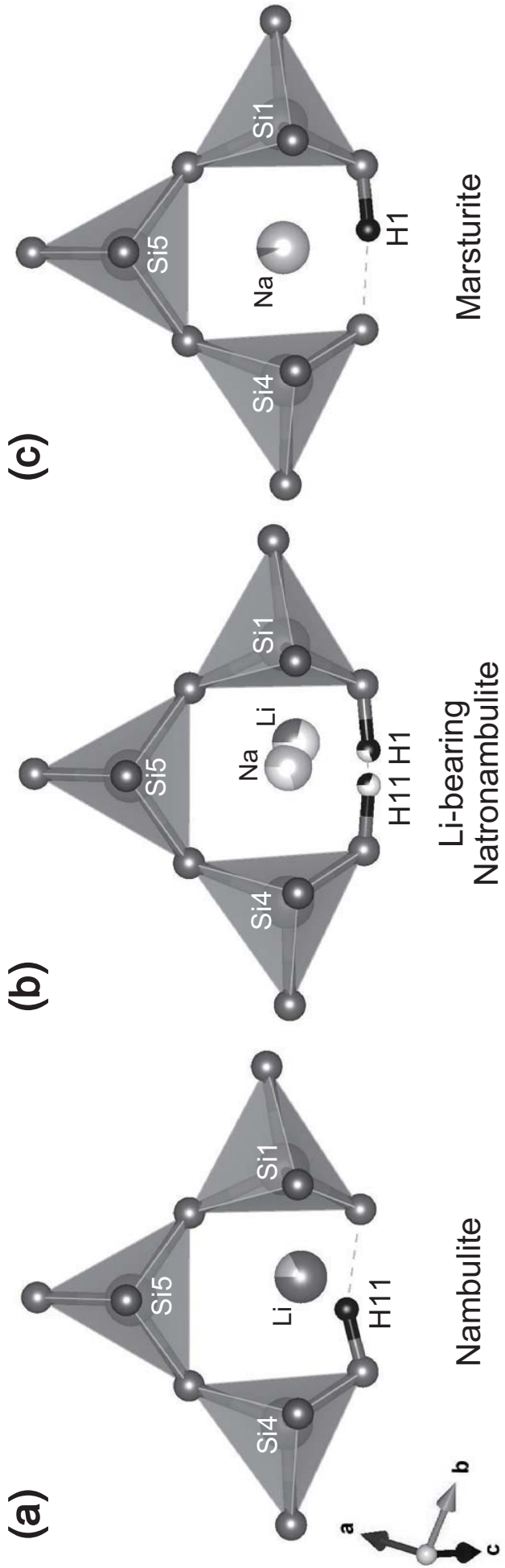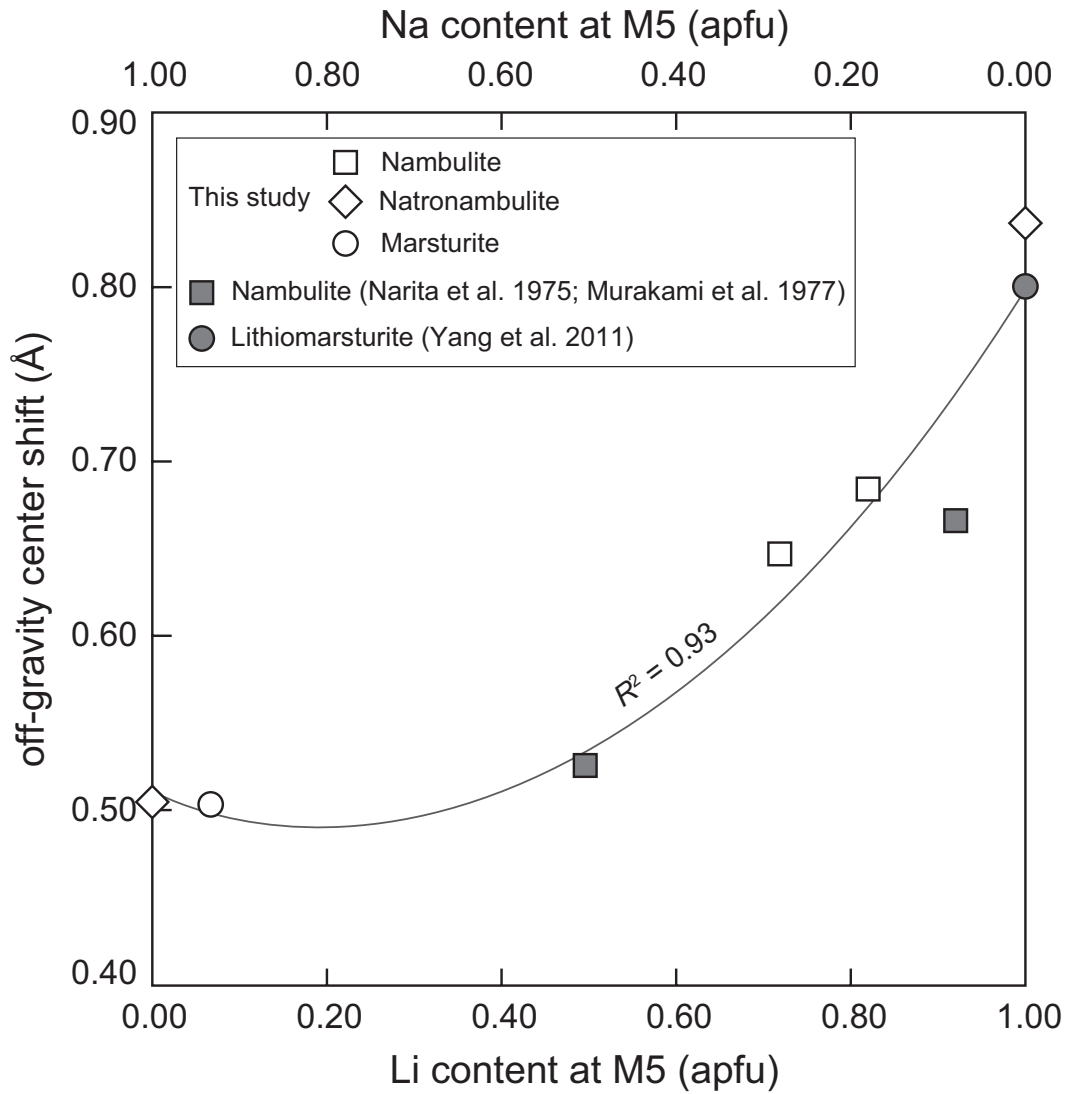
Figure 5

Figure 6

TABLE 1. Average chemical compositions of nambulite, natronambulite and marsturite*

wt.%	Nambulite[†] Fianel mine, Grisons, Switzerland (n = 21) Ave.	Std.	Nambulite[†] Gozaisho mine, Iwaki, Japan (n = 21) Ave.	Std.	Natronambulite[‡] Gozaisho mine, Iwaki, Japan (n = 24) Ave.	Std.	Marsturite[‡] Molinello mine, Liguria, Italy (n = 12) Ave.	Std.
SiO_2	48.42	0.44	50.08	0.24	49.06	0.29	49.36	0.35
As_2O_5	0.28	0.13	0.07	0.05	0.02	0.02	0.02	0.03
V_2O_5	0.22	0.09	0.01	0.01	0.01	0.01	0.17	0.16
TiO_2	0.04	0.06	0.04	0.04	0.01	0.01	0.01	0.01
Al_2O_3	0.02	0.02	0.01	0.01	0.01	0.01	0.01	0.01
Cr_2O_3	0.03	0.04	0.02	0.02	0.01	0.01	0.03	0.04
FeO	0.46	0.24	0.40	0.07	0.18	0.05	1.30	0.50
MnO	42.13	0.56	43.10	0.27	40.70	0.25	31.77	0.66
NiO	0.03	0.06	0.01	0.01	0.01	0.01	0.01	0.02
MgO	1.26	0.31	1.78	0.07	1.45	0.05	0.48	0.17
CaO	0.89	0.18	0.51	0.06	1.96	0.10	10.11	0.53
Na_2O	0.85	0.07	0.44	0.03	3.55	0.05	4.44	0.14
K_2O	0.01	0.01			0.01	0.01		
ZnO	0.13	0.12	0.01	0.02	0.02	0.04	0.02	0.02
Li_2O	1.88	0.15	2.19	0.05	1.13		0.33	
Total	96.65		98.67		98.13		98.06	
Cations								
Si	4.97	0.00	5.00	0.00	5.00	0.00	4.99	0.01
As^{5+}	0.02	0.01	0.00	0.00	0.00	0.00	0.00	0.00
V^{5+}	0.01	0.01	0.00	0.00	0.00	0.00	0.01	0.01
Ti	0.00	0.01	0.00	0.00	0.00	0.00	0.00	0.00
Al	0.00	0.00	0.00	0.00	0.00	0.00	0.00	0.00
Cr	0.00	0.00	0.00	0.00	0.00	0.00	0.00	0.00
Fe^{2+}	0.04	0.03	0.03	0.01	0.02	0.00	0.11	0.05
Mn^{2+}	3.66	0.06	3.64	0.03	3.51	0.03	2.72	0.33
Ni	0.00	0.01	0.00	0.00	0.00	0.00	0.00	0.00
Mg	0.19	0.03	0.26	0.01	0.22	0.01	0.07	0.07
Ca	0.10	0.02	0.05	0.01	0.21	0.01	1.09	0.36
Na	0.17	0.01	0.08	0.01	0.70	0.01	0.87	0.27
K	0.00	0.00	0.00	0.00	0.00	0.00	0.00	0.00
Zn	0.01	0.01	0.00	0.00	0.00	0.00	0.00	0.00
Li	0.60		0.67		0.36		0.10	
Total	9.78		9.76		10.02		9.96	

* Cation ratios are normalized as Si + As^{5+} + V^{5+} = 5.

[†] LiO_2 content was analyzed by LA-ICP-MS. Numbers of analytical points for Fianel and Gozaisho nambulite are 11 and 15, respectively.

[‡] LiO_2 content was calculated based on charge balance.

Table 2. Selected trace element concentrations of Fianel and Gozaisho nambulites

Fianel mine	Li (µg/g)	B (µg/g)	Al (µg/g)	P (µg/g)	Sc (µg/g)	Ti (µg/g)	V (µg/g)	Cr (µg/g)	Co (µg/g)	Ni (µg/g)	Cu (µg/g)	Zn (µg/g)	As (µg/g)	Sr (µg/g)	Y (µg/g)	Zr (µg/g)	Nb (µg/g)	Mo (µg/g)	Ba (µg/g)	La (µg/g)	Ce (µg/g)	Nd (µg/g)	Gd (µg/g)	Er (µg/g)	Yb (µg/g)	Hf (µg/g)	W (µg/g)	Pb (µg/g)	Th (µg/g)	U (µg/g)
1	9090	13.0	20.4	12.8	1.26	10.9	1520	<5.09	5.80	79	1.88	741	1440	2.99	21.1	1.50	0.06	<0.48	12.09	0.52	0.15	0.24	0.28	1.14	1.30	0.05	0.14	7.63	0.04	<0.05
2	8680	23.1	20.6	13.9	1.53	9.01	1030	<2.33	3.72	97	2.72	736	1540	5.31	26.4	9.62	0.04	<0.19	12.80	0.39	0.19	0.50	0.41	1.84	1.83	0.07	0.27	8.91	0.01	<0.02
3	8900	20.0	15.1	13.2	1.42	8.75	1080	<2.37	4.18	94	1.87	754	2100	4.41	28.5	9.40	0.03	<0.20	6.80	0.25	0.11	0.41	0.34	1.89	1.54	0.09	0.28	7.31	0.01	0.02
4	8590	25.8	24.3	10.7	1.44	11.3	1440	<2.27	3.72	109	1.74	782	1620	6.56	26.5	8.97	0.03	<0.18	17.16	0.63	0.20	0.44	0.40	1.70	1.41	0.07	0.35	13.1	<0.02	0.02
5	9180	29.7	25.5	11.2	1.06	8.48	801	4.24	4.23	147	2.54	756	791	11.7	26.9	3.31	0.05	<0.22	10.63	0.51	0.25	0.58	0.36	1.44	1.38	<0.02	1.14	16.7	<0.03	0.03
6	8200	9.70	18.2	<9.9	1.05	6.42	1130	<10.1	4.21	91	1.95	735	1260	2.73	24.4	3.92	<0.09	<0.78	10.73	0.48	0.10	<0.21	0.40	1.94	2.07	<0.11	0.16	6.61	<0.06	<0.06
7	8850	<11.44	11.3	<27.1	<2.00	<12.2	662	<28.3	4.76	124	<2.83	900	836	1.68	33.7	5.64	<0.30	<2.71	4.29	0.36	<0.21	<0.82	<0.85	3.31	1.04	<0.43	<0.57	4.66	<0.25	<0.24
8	8290	32.5	22.3	<24.0	<1.78	<9.1	1560	<24.8	4.88	104	2.56	792	1500	3.09	18.7	2.24	<0.28	<2.50	10.23	0.55	0.24	0.79	<0.56	1.51	1.14	<0.28	<0.37	6.23	<0.16	<0.16
9	8430	25.9	16.8	19.2	1.11	8.83	987	<9.5	3.41	99	1.49	695	1590	1.82	27.3	15.1	<0.06	<0.56	6.59	0.19	0.11	0.74	0.33	2.01	2.04	0.11	0.12	4.58	<0.03	<0.03
10	8350	6.82	12.7	11.1	1.30	9.35	636	<2.57	4.95	119	1.96	828	398	2.46	34.9	0.89	0.05	<0.15	1.41	0.33	0.18	0.45	0.55	2.11	1.45	<0.03	0.08	5.61	0.01	<0.02
11	9010	14.4	18.3	14.5	1.52	13.2	1090	<10.4	4.35	76	1.13	680	1310	1.89	23.4	4.61	<0.10	<1.02	8.41	0.32	0.19	0.38	0.85	1.48	0.84	<0.09	<0.23	5.44	<0.06	<0.05
Gozaisho mine	Li (µg/g)	B (µg/g)	Al (µg/g)	P (µg/g)	Sc (µg/g)	Ti (µg/g)	V (µg/g)	Cr (µg/g)	Co (µg/g)	Ni (µg/g)	Cu (µg/g)	Zn (µg/g)	As (µg/g)	Sr (µg/g)	Y (µg/g)	Zr (µg/g)	Nb (µg/g)	Mo (µg/g)	Ba (µg/g)	La (µg/g)	Ce (µg/g)	Nd (µg/g)	Gd (µg/g)	Er (µg/g)	Yb (µg/g)	Hf (µg/g)	W (µg/g)	Pb (µg/g)	Th (µg/g)	U (µg/g)
1	9960	13.8	144	8.77	5.49	7.07	2.20	7.33	364	77	248	91	73	0.69	21.9	5.67	0.05	<0.06	0.76	0.05	0.11	0.79	2.13	3.13	3.53	0.25	0.64	4.17	0.02	0.34
2	10320	5.98	28.4	8.45	5.08	5.80	1.51	6.69	349	72	356	80	114	0.64	20.3	4.30	0.01	<0.04	0.13	0.08	0.16	0.80	2.28	3.03	3.31	0.31	0.26	4.93	<0.005	0.04
3	10420	10.1	302	7.63	5.44	6.88	2.74	7.41	358	78	262	81	79	0.74	17.8	5.48	0.05	0.06	0.43	0.10	0.17	0.79	2.11	2.55	2.83	0.40	3.85	4.01	0.02	0.48
4	10560	6.05	50.4	9.58	5.35	8.48	2.15	5.28	344	72	371	78	134	0.49	21.8	5.79	<0.01	<0.10	0.10	0.03	0.09	0.81	2.32	3.31	3.64	0.31	0.27	1.58	<0.01	0.06
5	9820	14.2	358	8.25	5.39	7.87	4.08	5.68	321	74	288	80	133	0.72	18.7	4.09	0.05	<0.10	0.31	0.09	0.16	0.88	1.91	2.67	3.24	0.27	0.31	3.95	0.04	1.37
6	10030	5.00	24.4	7.2	4.59	11.1	1.02	11.1	343	74	233	90	40	0.61	20.7	2.34	<0.02	<0.07	0.21	0.05	0.12	0.83	2.39	3.04	3.09	0.09	0.16	3.36	<0.01	<0.01
7	10190	8.88	46.7	17.2	5.42	8.44	5.01	5.16	350	66	449	83	821	0.44	23.7	4.22	<0.02	0.05	0.66	0.03	0.12	0.90	2.11	3.62	4.44	0.18	<0.04	1.35	<0.01	0.13
8	10080	16.0	248	7.15	6.27	10.8	4.01	4.90	344	70	306	82	104	0.87	25.3	5.56	0.05	<0.03	0.33	0.06	0.18	0.99	2.49	3.80	4.38	0.21	0.43	7.28	<0.0	1.35
9	10260	10.9	14.4	13.3	5.26	8.20	3.73	4.83	345	70	346	88	939	0.61	22.8	3.51	<0.02	<0.06	0.61	0.05	0.10	0.71	2.29	3.32	3.80	0.19	0.19	3.32	0.01	<0.01
10	10440	10.3	18.4	12.9	5.54	7.98	3.20	5.95	353	71	402	87	946	0.67	25.2	3.69	<0.02	0.05	0.65	0.05	0.13	0.81	2.57	3.68	4.51	0.19	0.07	2.73	0.02	0.02
11	9890	8.30	78.4	7.53	5.77	10.0	3.33	6.74	342	69	249	85	97	1.33	30.7	6.15	0.05	<0.13	2.85	0.12	0.25	1.22	3.36	4.68	5.29	0.25	1.05	8.76	0.06	0.15
12	9910	11.4	212	11.2	5.55	0.10	3.67	7.79	346	70	219	85	604	0.91	21.9	3.69	0.04	<0.11	0.72	0.15	0.22	0.87	2.46	3.16	3.60	0.12	0.56	9.01	0.04	0.39
13	10540	7.46	92.2	7.02	5.36	5.64	1.45	6.87	355	75	260	78	62	0.57	20.4	4.60	0.03	<0.09	<0.13	0.07	0.12	0.79	2.08	3.08	3.55	0.24	0.11	2.60	0.02	0.29
14	10150	7.79	48.9	9.14	5.61	8.39	2.67	6.33	345	74	430	81	154	0.52	22.5	5.83	<0.01	<0.10	0.26	0.02	0.11	0.83	2.41	3.22	3.73	0.29	0.06	1.80	<0.01	0.10
15	10030	6.16	42.3	6.23	5.16	5.55	1.53	6.25	341	77	383	73	84	0.56	18.4	4.32	<0.01	<0.11	<0.16	0.02	0.10	0.74	2.13	2.68	3.08	0.29	0.07	2.52	<0.01	0.05

TABLE 3. Experimental details of the single-crystal X-ray diffraction analysis of nambulite, natronambulite and marsturite samples[*].

	Nambulite		Natronambulite	Marsturite[†]
	Fianel mine, Grisons, Switzerland	Gozaisho mine, Iwaki, Japan	Gozaisho mine, Iwaki, Japan	Molinello mine, Liguria, Italy
Crystal size (mm)	0.035 × 0.025 × 0.02	0.27 × 0.10 × 0.06	0.27 × 0.10 × 0.06	0.17 × 0.12 × 0.08
Space group	$P\bar{1}$		$P\bar{1}$	$P\bar{1}$
Cell parameters a (Å)	7.5391(2)	7.5372(1)	7.6115(1)	7.697(2)
b (Å)	11.7475(3)	11.7267(1)	11.7340(2)	11.720(2)
c (Å)	6.7137(2)	6.7078(1)	6.7324(1)	6.771(1)
α (°)	93.024(2)	93.057(1)	92.876(1)	92.40(3)
β (°)	95.147(2)	95.147(1)	94.846(1)	94.41(3)
γ (°)	106.266(2)	106.240(1)	106.650(1)	106.83(3)
V (Å^3)	566.61(4)	565.02(2)	572.28(2)	581.9(6)
D_{calc} (g/cm^3)[‡]	3.55	3.54	3.54	3.47
Radiation	Mo$K\alpha$ (λ = 0.71069Å)			
Monochrometer	Graphite			
Diffractometer	Bruker SMART APEXII CCD			Nonius KappaCCD
Scan type	φ-ω scan (Bruker 1999)			φ-ω scan
θ_{min}(°)	1.8	2.8	1.8	2.8
θ_{max}(°)	30.5	30.5	30.5	30.1
μ (mm^{-1})	4.90	4.85	4.67	4.31
Collected reflections	13031	12760	24804	6444
Unique reflctions	3409	3420	3484	3371
R_{int} (%)	3.55	1.38	1.74	3.48
R_{σ} (%)	2.96	1.24	1.00	5.09
Miller index limits	-10 < h < 10, -16 < k < 16, -9 < l < 9	-10 < h < 10, -16 < k < 16, -9 < l < 9	-10 < h < 10, -16 < k < 16, -9 < l < 9	-10 < h < 10, -16 < k < 16, -9 < l < 9
Refinement system used	SHELXL-97 (Sheldrick 2008)			
R_1 (%)	3.90	1.74	1.56	5.53
wR_2 (%)	10.31	6.82	4.63	14.18
No. of parameters	231	231	239	233
Weighting scheme*	$w = 1/[\sigma^2(F_o^2) + (0.0547P)^2 + 1.54P]$	$w = 1/[\sigma^2(F_o^2) + (0.0324P)^2 + 0.60P]$	$w = 1/[\sigma^2(F_o^2) + (0.0232P)^2 + 0.34P]$	$w = 1/[\sigma^2(F_o^2) + (0.0560P)^2 + 3.08P]$
Δr_{max} (e Å^{-3})	2.46 (0.74 Å from M2)	0.58 (0.71 Å from O3)	0.45 (0.55 Å from O3)	1.65 (1.33 Å from O13)
Δr_{min} (e Å^{-3})	-0.61 (0.69 Å from M2)	-0.67 (0.18 Å from M1)	-0.47 (0.61 Å from M4)	-0.92 (0.82 Å from M1)

[*] The function of the weighting scheme is $w = 1/(\sigma^2(F_o^2) + (a \cdot P)^2 + b \cdot P)$, where $P = (\text{Max}(F_o^2) + 2F_c^2)/3$, and the parameters a and b are chosen to minimize the diffrerences in the variances for reflections in different ranges of intensity and diffraction angle.

[†] The accuracies of unit-cell parameters had been empirically multiplied by 10. Collected reflections actually represent the merged number.

[‡] Density (g/cm^3) was calculated using the determined site occupancies in this study.

TABLE 4. Refined atomic positions and isotropic mean square displacement parameters (Å²) of the nambulite and marsturite samples

Site	neq*	W†		Nambulite Fianel, Switzerland	Nambulite Gozaisho, Japan	Natronambulite Gozaisho, Japan	Marsturite Molinello, Italy
M1	2	i	x	0.59457(7)	0.59473(4)	0.59207(3)	0.59347(11)
			y	0.65350(4)	0.65395(2)	0.653701(17)	0.64999(7)
			z	0.06068(7)	0.06110(4)	0.06309(3)	0.06289(11)
			U_{eq}	0.00995(12)	0.00945(7)	0.00988(5)	0.0182(2)
M2	2	i	x	0.81481(7)	0.81507(4)	0.80995(3)	0.80504(12)
			y	0.94088(4)	0.94164(2)	0.941407(17)	0.940011(8)
			z	0.12908(7)	0.12933(4)	0.12595(4)	0.12446(12)
			U_{eq}	0.01211(13)	0.00930(7)	0.00992(5)	0.0195(3)
M3	2	i	x	0.03859(7)	0.03828(4)	0.04032(3)	0.03951(11)
			y	0.23512(5)	0.23486(3)	0.235201(18)	0.23533(7)
			z	0.18048(8)	0.17946(5)	0.17572(3)	0.17309(12)
			U_{eq}	0.00978(17)	0.00942(11)	0.00907(7)	0.0175(3)
M4	2	i	x	0.24687(7)	0.24670(4)	0.24236(3)	0.23215(14)
			y	0.51374(5)	0.51372(3)	0.51541(2)	0.52332(10)
			z	0.26525(7)	0.26589(4)	0.26632(3)	0.27776(15)
			U_{eq}	0.01218(16)	0.01148(10)	0.01396(7)	0.0235(3)
M5	2	i	x	0.6726(8)	0.6665(5)	0.67662(13) for Na 0.645(2) for Li	0.6753(3)
			y	0.1108(5)	0.1202(4)	0.14334(10) for Na 0.112(1) for Li	0.1466(2)
			z	0.3628(9)	0.3488(6)	0.37012(15) for Na 0.328(2) for Li	0.3710(4)
			U_{eq}	0.055(2)	0.0432(12)	0.0186(3)	0.0299(9)
Si1	2	i	x	0.28019(12)	0.27910(6)	0.27118(5)	0.2670(2)
			y	0.05957(8)	0.05960(4)	0.05933(3)	0.05745(13)
			z	0.35765(13)	0.35814(7)	0.35868(5)	0.3557(2)
			U_{eq}	0.00960(18)	0.00649(10)	0.00779(7)	0.0185(3)
Si2	2	i	x	0.47475(11)	0.47395(6)	0.46769(5)	0.4577(2)
			y	0.32697(7)	0.32678(4)	0.32896(3)	0.32818(13)
			z	0.42820(12)	0.42779(7)	0.42677(5)	0.4251(2)
			U_{eq}	0.00699(16)	0.00658(10)	0.00794(7)	0.0159(3)
Si3	2	i	x	0.81894(11)	0.81858(6)	0.81426(4)	0.80561(19)
			y	0.45595(7)	0.45512(4)	0.45278(3)	0.45012(13)
			z	0.22172(12)	0.22094(7)	0.21928(5)	0.2169(2)
			U_{eq}	0.00653(16)	0.00666(10)	0.00730(7)	0.0149(3)
Si4	2	i	x	0.00894(12)	0.00911(7)	0.00041(4)	-0.0055(2)
			y	0.72550(7)	0.72515(4)	0.72396(3)	0.72249(13)
			z	0.30111(12)	0.30072(7)	0.30440(5)	0.3073(2)
			U_{eq}	0.00798(17)	0.00685(10)	0.00734(7)	0.0163(3)
Si5	2	i	x	0.35105(11)	0.35079(6)	0.34520(4)	0.34147(19)
			y	0.85360(7)	0.85358(4)	0.85400(3)	0.85220(13)
			z	0.11409(12)	0.11427(7)	0.12056(5)	0.1220(2)
			U_{eq}	0.00694(17)	0.00665(10)	0.00749(7)	0.0166(3)
O1	2	i	x	0.1991(3)	0.20002(19)	0.18836(13)	0.1808(5)
			y	0.0096(2)	0.00859(12)	0.00843(8)	0.0096(4)
			z	0.5608(3)	0.56108(19)	0.56095(14)	0.5589(6)
			U_{eq}	0.0149(5)	0.0117(2)	0.01305(18)	0.0238(8)
O2	2	i	x	0.1205(3)	0.12134(18)	0.11946(12)	0.1169(5)
			y	0.0682(2)	0.06896(12)	0.06725(8)	0.0651(5)
			z	0.1861(3)	0.18570(19)	0.18303(13)	0.1814(5)
			U_{eq}	0.0120(4)	0.0090(2)	0.00978(16)	0.0209(8)
O3	2	i	x	0.4468(3)	0.44631(18)	0.42790(14)	0.4176(5)
			y	0.1830(2)	0.18254(11)	0.18450(8)	0.1831(3)
			z	0.4173(3)	0.4172(2)	0.42510(15)	0.4264(5)
			U_{eq}	0.0127(4)	0.0105(2)	0.0165(2)	0.0203(8)
O4	2	i	x	0.3288(3)	0.32764(18)	0.32721(12)	0.3230(5)
			y	0.3497(2)	0.34914(12)	0.35159(8)	0.3525(3)
			z	0.2544(3)	0.25387(19)	0.25068(14)	0.2491(5)
			U_{eq}	0.0093(4)	0.0091(2)	0.01014(17)	0.0176(7)
O5	2	i	x	0.5290(3)	0.53014(19)	0.52935(13)	0.5399(5)
			y	0.6165(2)	0.61611(12)	0.61187(9)	0.6124(3)
			z	0.3520(3)	0.35240(19)	0.35476(14)	0.3592(5)
			U_{eq}	0.0117(4)	0.0107(2)	0.01261(17)	0.0210(8)
O6	2	i	x	0.6941(3)	0.69321(18)	0.68649(12)	0.6771(5)
			y	0.3839(2)	0.38359(12)	0.37629(9)	0.3731(3)
			z	0.3879(4)	0.3878(2)	0.38082(14)	0.3776(5)
			U_{eq}	0.0132(4)	0.0114(2)	0.01264(18)	0.0198(8)
O7	2	i	x	0.9797(3)	0.97941(19)	0.97520(13)	0.9590(5)
			y	0.3976(2)	0.39692(13)	0.39628(9)	0.3909(4)
			z	0.1737(3)	0.1734(2)	0.17223(15)	0.1655(6)
			U_{eq}	0.01244	0.0127(2)	0.01464(19)	0.0231(8)
O8	2	i	x	0.6806(3)	0.67970(18)	0.67927(12)	0.6763(5)
			y	0.4708(2)	0.46980(12)	0.46847(8)	0.4707(3)
			z	0.0339(3)	0.0335(2)	0.03237(14)	0.0329(5)
			U_{eq}	0.0098(4)	0.0103(2)	0.01050(17)	0.0172(7)
O9	2	i	x	0.9330(4)	0.93241(19)	0.92518(13)	0.9226(5)
			y	0.5859(2)	0.58563(11)	0.58268(8)	0.5781(3)
			z	0.3363(3)	0.3368(2)	0.33770(14)	0.3386(5)
			U_{eq}	0.0138(5)	0.0126(2)	0.01334(18)	0.0221(8)
O10	2	i	x	0.8813(3)	0.88200(18)	0.87607(12)	0.8741(5)
			y	0.7671(2)	0.76755(12)	0.76526(8)	0.7636(3)
			z	0.1307(3)	0.1304(2)	0.13216(14)	0.1349(5)
			U_{eq}	0.0103(4)	0.0096(2)	0.00959(16)	0.0180(7)
O11	2	i	x	-0.0241(4)	-0.0227(2)	-0.01209(14)	-0.0069(5)
			y	0.2026(2)	0.20339(12)	0.20530(8)	0.2080(3)
			z	0.4827(3)	0.4825(2)	0.48146(14)	0.4810(5)
			U_{eq}	0.0157(5)	0.0147(3)	0.01360(18)	0.0212(8)
O12	2	i	x	0.2178(3)	0.21798(18)	0.21059(12)	0.2060(5)
			y	0.7457(2)	0.74572(12)	0.74522(8)	0.7440(3)
			z	0.2282(4)	0.2299(2)	0.23715(14)	0.2411(5)
			U_{eq}	0.0143(5)	0.0113(2)	0.01179(17)	0.0208(8)
O13	2	i	x	0.5376(3)	0.53802(18)	0.53060(12)	0.5260(5)
			y	0.8233(2)	0.82382(12)	0.82388(8)	0.8214(3)
			z	0.0693(4)	0.0706(2)	0.07655(14)	0.0784(5)
			U_{eq}	0.0120(4)	0.0097(2)	0.01090(17)	0.0224(8)
O14	2	i	x	0.7653(3)	0.76642(18)	0.77051(13)	0.7707(5)
			y	0.1196(2)	0.12076(12)	0.11940(8)	0.1188(3)
			z	0.0847(3)	0.08387(19)	0.07460(14)	0.0713(5)
			U_{eq}	0.0109(4)	0.0100(2)	0.01116(17)	0.0199(8)
O15	2	i	x	0.3996(3)	0.39871(18)	0.39211(13)	0.3887(5)
			y	0.9728(2)	0.97295(12)	0.97274(8)	0.9707(3)
			z	0.2753(2)	0.2733(2)	0.28226(14)	0.2839(5)
			U_{eq}	0.0137(5)	0.0114(2)	0.01218(17)	0.0216(8)
H1	2	i	x			0.112(5)	0.093(8)
			y			-0.0749(11)	-0.074(3)
			z			0.544(7)	0.535(11)
			U_{iso}			0.05	0.05
H11	2	i	x		-0.107(4)	-0.053(13)	
			y		0.1242(16)	0.11788(15)	
			z		0.494(6)	0.471(16)	
			U_{iso}		0.05	0.05	

* Multiplicity
† Wyckoff letter

TABLE 5. Anisotropic mean square displacement parameters (Å^2) of the nambulite, natronambulite and marsturite samples

Site		Nambulite Fianel, Switzerland	Nambulite Gozaisho, Japan	Natronambulite Gozaisho, Japan	Marsturite Molinello, Italy
M1	U_{11}	0.0078(2)	0.00884(13)	0.00860(9)	0.0162(4)
	U_{22}	0.0104(2)	0.00998(13)	0.01079(9)	0.0219(4)
	U_{33}	0.0102(2)	0.00884(12)	0.00917(9)	0.0153(4)
	U_{23}	0.00035(15)	0.00067(9)	0.00097(7)	0.0010(3)
	U_{13}	0.00033(15)	0.00118(9)	0.00129(6)	0.0003(3)
	U_{12}	0.00042(17)	0.00150(9)	0.00098(7)	0.0039(3)
M2	U_{11}	0.0117(2)	0.00988(13)	0.01043(9)	0.0215(5)
	U_{22}	0.0104(2)	0.00879(13)	0.00954(9)	0.0203(5)
	U_{33}	0.0133(2)	0.00908(13)	0.00970(10)	0.0167(4)
	U_{23}	-0.00034(16)	0.00018(9)	0.00050(7)	-0.0002(3)
	U_{13}	-0.00005(17)	0.00179(9)	0.00196(7)	-0.0003(3)
	U_{12}	0.00242(18)	0.00231(10)	0.00258(7)	0.0067(3)
M3	U_{11}	0.0081(3)	0.00901(16)	0.00878(11)	0.0167(5)
	U_{22}	0.0082(3)	0.00867(17)	0.00843(11)	0.0195(5)
	U_{33}	0.0117(3)	0.01043(16)	0.00972(11)	0.0155(4)
	U_{23}	-0.00025(16)	0.00049(10)	0.00079(7)	0.0001(3)
	U_{13}	-0.00016(17)	0.00100(11)	0.00117(7)	0.0013(3)
	U_{12}	0.00076(18)	0.00235(11)	0.00198(7)	0.0045(3)
M4	U_{11}	0.0087(3)	0.00960(15)	0.01114(10)	0.0201(6)
	U_{22}	0.0118(3)	0.01167(16)	0.01402(11)	0.0244(6)
	U_{33}	0.0131(3)	0.01110(15)	0.01337(11)	0.0218(5)
	U_{23}	-0.00137(16)	-0.00033(10)	0.00102(8)	0.0001(4)
	U_{13}	-0.00134(17)	-0.00033(10)	-0.00135(7)	-0.0039(4)
	U_{12}	-0.00067(18)	0.00033(10)	-0.00088(8)	0.0018(4)
M5	U_{11}	0.051(3)	0.043(2)	0.0110(5)	0.0198(14)
	U_{22}	0.050(3)	0.058(2)	0.0271(6)	0.0438(17)
	U_{33}	0.058(4)	0.045(2)	0.0159(5)	0.0258(14)
	U_{23}	-0.007(2)	0.0217(16)	-0.0017(3)	-0.0042(11)
	U_{13}	0.042(3)	0.0296(15)	0.0025(3)	0.0048(10)
	U_{12}	-0.001(3)	0.0300(17)	0.0029(4)	0.0091(11)
Si1	U_{11}	0.0087(4)	0.0068(2)	0.00890(14)	0.0200(7)
	U_{22}	0.0073(4)	0.0058(2)	0.00650(14)	0.0191(7)
	U_{33}	0.0108(4)	0.00664(19)	0.00737(15)	0.0157(7)
	U_{23}	-0.0002(3)	0.00030(15)	0.00048(11)	0.0016(5)
	U_{13}	-0.0015(3)	0.00002(15)	0.00023(11)	0.0001(5)
	U_{12}	0.0002(3)	0.00153(15)	0.00152(11)	0.0050(6)
Si2	U_{11}	0.0063(4)	0.0069(2)	0.00906(14)	0.0177(7)
	U_{22}	0.0054(4)	0.0062(2)	0.00698(14)	0.0171(7)
	U_{33}	0.0078(3)	0.0060(2)	0.00650(15)	0.0119(6)
	U_{23}	0.0002(2)	0.00066(15)	0.00098(11)	0.0007(5)
	U_{13}	-0.0004(3)	0.00016(15)	0.00042(11)	-0.0008(5)
	U_{12}	-0.0002(3)	0.00096(15)	0.00034(11)	0.0040(6)

Site		Nambulite Fianel, Switzerland	Nambulite Gozaisho, Japan	Natronambulite Gozaisho, Japan	Marsturite Molinello, Italy
Si3	U_{11}	0.0041(3)	0.0060(2)	0.00693(14)	0.0151(7)
	U_{22}	0.0057(3)	0.0066(2)	0.00734(14)	0.0171(7)
	U_{33}	0.0086(3)	0.0073(2)	0.00770(15)	0.0128(6)
	U_{23}	0.0012(3)	0.00131(15)	0.00151(11)	0.0019(5)
	U_{13}	-0.0002(3)	0.00075(15)	0.00108(11)	0.0008(5)
	U_{12}	-0.0004(3)	0.00151(15)	0.00197(11)	0.0050(5)
Si4	U_{11}	0.0067(4)	0.0068(2)	0.00744(14)	0.0159(7)
	U_{22}	0.0063(4)	0.0061(2)	0.00653(14)	0.0193(7)
	U_{33}	0.0096(3)	0.0072(2)	0.00758(15)	0.0134(6)
	U_{23}	-0.0001(3)	0.00060(15)	0.00048(11)	0.0006(5)
	U_{13}	-0.0007(3)	0.00038(15)	0.00013(11)	-0.0004(5)
	U_{12}	0.0003(3)	0.00126(15)	0.00148(11)	0.0049(6)
Si5	U_{11}	0.0048(3)	0.0062(2)	0.00681(14)	0.0162(7)
	U_{22}	0.0071(4)	0.0072(2)	0.00856(15)	0.0187(7)
	U_{33}	0.0082(3)	0.00669(19)	0.00727(15)	0.0145(6)
	U_{23}	-0.0009(3)	0.00023(15)	0.00054(11)	0.0002(5)
	U_{13}	-0.0006(3)	0.00052(15)	0.00044(11)	0.0011(5)
	U_{12}	0.0012(3)	0.00213(15)	0.00262(11)	0.0048(6)
O1	U_{11}	0.0146(11)	0.0128(6)	0.0165(4)	0.023(2)
	U_{22}	0.0150(11)	0.0125(6)	0.0123(4)	0.025(2)
	U_{33}	0.0123(10)	0.0080(5)	0.0088(4)	0.0208(19)
	U_{23}	0.0030(8)	0.0017(4)	0.0018(3)	0.0038(16)
	U_{13}	0.0013(8)	0.0016(4)	0.0032(3)	0.0024(15)
	U_{12}	-0.0007(9)	0.0006(5)	0.0011(3)	0.0022(17)
O2	U_{11}	0.0092(10)	0.0084(5)	0.0102(4)	0.023(2)
	U_{22}	0.0115(10)	0.0111(6)	0.0118(4)	0.024(2)
	U_{33}	0.0134(10)	0.0079(5)	0.0079(4)	0.0156(17)
	U_{23}	-0.0011(8)	0.0007(4)	0.0006(3)	0.0008(14)
	U_{13}	-0.0039(8)	0.0000(4)	0.0000(3)	-0.0007(14)
	U_{12}	0.0021(8)	0.0037(4)	0.0044(3)	0.0071(16)
O3	U_{11}	0.0124(11)	0.0111(6)	0.0211(5)	0.021(2)
	U_{22}	0.0058(10)	0.0061(5)	0.0072(4)	0.0178(18)
	U_{33}	0.0167(10)	0.0128(6)	0.0162(5)	0.0205(18)
	U_{23}	-0.0008(7)	0.0006(4)	0.0020(3)	0.0021(14)
	U_{13}	-0.0032(8)	-0.0013(4)	-0.0061(4)	-0.0009(14)
	U_{12}	-0.0008(8)	0.0006(4)	-0.0016(3)	0.0039(15)

Site		Nambulite Fianel, Switzerland	Nambulite Gozaisho, Japan	Natronambulite Gozaisho, Japan	Marsturite Molinello, Italy
O4	U_{11}	0.0074(10)	0.0089(5)	0.0093(4)	0.0161(18)
	U_{22}	0.0097(10)	0.0099(6)	0.0116(4)	0.0215(19)
	U_{33}	0.0101(9)	0.0084(5)	0.0090(4)	0.0141(16)
	U_{23}	0.0003(7)	0.0011(4)	0.0014(3)	-0.0002(13)
	U_{13}	-0.0011(7)	-0.0005(4)	0.0002(3)	0.0007(13)
	U_{12}	0.0017(8)	0.0031(4)	0.0023(3)	0.0044(15)
O5	U_{11}	0.0111(10)	0.0129(6)	0.0147(4)	0.022(2)
	U_{22}	0.0137(11)	0.0113(6)	0.0141(4)	0.022(2)
	U_{33}	0.0082(9)	0.0076(5)	0.0083(4)	0.0167(17)
	U_{23}	-0.0021(7)	-0.0010(4)	-0.0004(3)	-0.0005(14)
	U_{13}	0.0005(7)	0.0012(4)	0.0017(3)	0.0026(14)
	U_{12}	0.0008(8)	0.0032(5)	0.0031(3)	0.0042(16)
O6	U_{11}	0.0064(10)	0.0078(5)	0.0091(4)	0.0166(18)
	U_{22}	0.0155(11)	0.0134(6)	0.0160(4)	0.026(2)
	U_{33}	0.0158(10)	0.0125(6)	0.0133(4)	0.0163(17)
	U_{23}	0.0069(8)	0.0063(5)	0.0072(3)	0.0068(14)
	U_{13}	0.0013(8)	0.0020(4)	0.0026(3)	0.0024(14)
	U_{12}	-0.0006(8)	0.0012(4)	0.0032(3)	0.0042(15)
O7	U_{11}	0.0099(10)	0.0110(6)	0.0144(4)	0.026(2)
	U_{22}	0.0129(11)	0.0137(6)	0.0158(5)	0.026(2)
	U_{33}	0.0156(10)	0.0152(6)	0.0171(5)	0.0221(19)
	U_{23}	0.0004(8)	0.0013(5)	0.0030(4)	0.0041(15)
	U_{13}	0.0024(8)	0.0024(5)	0.0051(3)	0.0054(15)
	U_{12}	0.0053(9)	0.0061(5)	0.0086(4)	0.0140(17)
O8	U_{11}	0.0066(10)	0.0090(5)	0.0092(4)	0.0179(18)
	U_{22}	0.0108(10)	0.0128(6)	0.0128(4)	0.0183(18)
	U_{33}	0.0099(9)	0.0081(5)	0.0087(4)	0.0144(16)
	U_{23}	0.0004(7)	0.0017(4)	0.0018(3)	-0.0003(13)
	U_{13}	-0.0025(7)	-0.0013(4)	-0.0004(3)	-0.0006(13)
	U_{12}	0.0001(8)	0.0022(5)	0.0020(3)	0.0043(15)
O9	U_{11}	0.0168(12)	0.0151(6)	0.0156(4)	0.027(2)
	U_{22}	0.0055(10)	0.0061(5)	0.0076(4)	0.0201(19)
	U_{33}	0.0138(10)	0.0130(6)	0.0136(4)	0.0172(17)
	U_{23}	0.0008(7)	0.0015(4)	0.0012(3)	0.0001(14)
	U_{13}	-0.0056(8)	-0.0035(5)	-0.0032(3)	-0.0051(15)
	U_{12}	-0.0032(8)	-0.0014(5)	-0.0004(3)	0.0055(16)

Site		Nambulite Fianel, Switzerland	Nambulite Gozaisho, Japan	Natronambulite Gozaisho, Japan	Marsturite Molinello, Italy
O10	U_{11}	0.0076(10)	0.0085(5)	0.0082(4)	0.0170(18)
	U_{22}	0.0100(10)	0.0106(6)	0.0109(4)	0.0211(19)
	U_{33}	0.0134(10)	0.0102(6)	0.0098(4)	0.0151(16)
	U_{23}	0.0018(7)	0.0020(4)	0.0020(3)	0.0011(14)
	U_{13}	-0.0010(8)	0.0002(4)	0.0001(3)	0.0001(13)
	U_{12}	0.0030(8)	0.0037(4)	0.0031(3)	0.0049(15)
O11	U_{11}	0.0249(13)	0.0244(7)	0.0197(5)	0.025(2)
	U_{22}	0.0090(11)	0.0092(6)	0.0100(4)	0.022(2)
	U_{33}	0.0121(10)	0.0091(6)	0.0096(4)	0.0161(17)
	U_{23}	-0.0006(8)	-0.0008(4)	-0.0010(3)	0.0003(14)
	U_{13}	0.0025(9)	0.0032(5)	0.0028(3)	0.0012(14)
	U_{12}	0.0031(9)	0.0023(5)	0.0018(3)	0.0062(16)
O12	U_{11}	0.0077(10)	0.0074(5)	0.0079(4)	0.0197(19)
	U_{22}	0.0184(12)	0.0138(6)	0.0146(4)	0.026(2)
	U_{33}	0.0161(10)	0.0133(6)	0.0136(4)	0.0176(17)
	U_{23}	0.0058(8)	0.0051(5)	0.0055(3)	0.0024(15)
	U_{13}	0.0015(8)	0.0023(4)	0.0024(3)	0.0007(14)
	U_{12}	0.0020(9)	0.0030(4)	0.0032(3)	0.0084(16)
O13	U_{11}	0.0081(10)	0.0079(5)	0.0083(4)	0.021(2)
	U_{22}	0.0100(10)	0.0087(6)	0.0107(4)	0.026(2)
	U_{33}	0.0178(11)	0.0132(6)	0.0144(4)	0.0209(18)
	U_{23}	0.0019(8)	0.0005(4)	0.0010(3)	0.0030(15)
	U_{13}	0.0020(8)	0.0028(4)	0.0029(3)	0.0034(15)
	U_{12}	0.0021(8)	0.0033(4)	0.0034(3)	0.0076(16)
O14	U_{11}	0.0084(10)	0.0104(6)	0.0115(4)	0.0181(19)
	U_{22}	0.0116(10)	0.0106(6)	0.0113(4)	0.0209(19)
	U_{33}	0.0112(9)	0.0090(5)	0.0101(4)	0.0192(17)
	U_{23}	0.0017(7)	0.0019(4)	0.0020(3)	0.0004(14)
	U_{13}	-0.0030(7)	-0.0009(4)	-0.0020(3)	-0.0031(14)
	U_{12}	0.0013(8)	0.0035(4)	0.0031(3)	0.0048(15)
O15	U_{11}	0.0120(11)	0.0111(6)	0.0117(4)	0.022(2)
	U_{22}	0.0107(11)	0.0115(6)	0.0121(4)	0.022(2)
	U_{33}	0.0167(10)	0.0121(6)	0.0131(4)	0.0207(18)
	U_{23}	-0.0065(8)	-0.0031(4)	-0.0030(3)	-0.0054(15)
	U_{13}	-0.0041(8)	-0.0015(4)	-0.0017(3)	-0.0039(15)
	U_{12}	0.0036(9)	0.0058(5)	0.0054(3)	0.0095(16)

TABLE 6. Number of electrons and cation assignments*

Site	Observed number of e⁻	Occupancy	Calculated number of e⁻
Nambulite			
Fianel mine, Grisons, Switzerland			
M1	25 (fix)	Mn1.0	25
M2	25 (fix)	Mn1.0	25
M3	23.19	Mn0.81+Mg0.19	22.53
M4	24.69	Mn0.90+Ca0.10	24.50
M5	5.20	Na0.28+Li0.72	5.20
Gozaisho mine, Iwaki, Japan			
M1	25 (fix)	Mn1.0	25
M2	25 (fix)	Mn1.0	25
M3	21.84	Mn0.74+Mg0.26	21.62
M4	24.53	Mn0.95+Ca0.05	24.75
M5	4.43	Na0.18+Li0.82	4.43
Natronambulite			
Gozaisho mine, Iwaki, Japan			
M1	25 (fix)	Mn1.0	25
M2	25 (fix)	Mn1.0	25
M3	22.79	Mn0.78+Mg0.22	22.14
M4	23.95	Mn0.79+Ca0.21	23.95
M5	8.76	Na0.72+Li0.28	8.76
Marsturite			
Molinello mine, Liguria, Italy			
M1	25 (fix)	Mn1.0	25
M2	24.25	Mn0.85+Ca0.15	24.25
M3	24.35	Mn0.82+Fe0.11+Mg0.07	24.20
M4	21.20	Ca0.76+Mn0.24	21.20
M5	10.52	Na0.94+Li0.06	10.52

* Mg and Ca contents in nambulite and natronambulite, and Mg and Fe contents in marsturite are fixed by EMPA data. Mn and Ca occupancies at M2 and M4 in marsturite, and Na and Li occupancies in M5 in all samples are derived from the results of structural refinement.

TABLE 7. Selected bond distances (Å)

	Nambulite	Nambulite	Natronambulite	Marsturite
	Fianel, Switzerland	Gozaisho, Japan	Gozaisho, Japan	Molinello, Italy
M1- O4	2.244(2)	2.243(1)	2.2521(9)	2.256(4)
O5	2.098(2)	2.096(1)	2.108(1)	2.118(4)
O8	2.412(2)	2.421(1)	2.452(1)	2.372(4)
O8'	2.193(2)	2.185(1)	2.1726(9)	2.179(4)
O10	2.193(2)	2.195(1)	2.1795(9)	2.190(4)
O13	2.154(2)	2.150(1)	2.1769(9)	2.216(4)
Mean (VI)	2.216	2.215	2.224	2.222
M2- O1	2.152(2)	2.146(1)	2.158(1)	2.194(4)
O2	2.355(2)	2.357(1)	2.3822(9)	2.415(4)
O2'	2.218(2)	2.213(1)	2.1966(1)	2.204(4)
O10	2.234(2)	2.236(1)	2.2646(9)	2.283(4)
O13	2.147(2)	2.146(1)	2.1651(9)	2.186(4)
O14	2.263(2)	2.262(1)	2.2329(9)	2.226(4)
Mean (VI)	2.228	2.227	2.233	2.251
M3- O2	2.216(2)	2.205(1)	2.2213(9)	2.243(4)
O4	2.220(2)	2.214(1)	2.2189(9)	2.224(4)
O7	2.080(2)	2.071(1)	2.088(1)	2.090(4)
O10	2.227(2)	2.216(1)	2.2193(9)	2.237(4)
O11	2.154(3)	2.153(1)	2.156(1)	2.163(4)
O14	2.146(2)	2.131(1)	2.1446(1)	2.165(4)
Mean(VI)	2.174	2.165	2.175	2.187
M4- O4	2.182(2)	2.180(1)	2.1968(9)	2.310(4)
O5	2.141(2)	2.147(1)	2.169(1)	2.307(4)
O6	2.507(3)	2.502(1)	2.576(1)	2.536(4)
O7	2.109(3)	2.112(1)	2.134(1)	2.274(4)
O8	2.132(2)	2.135(1)	2.147(1)	2.266(4)
O9	2.798(3)	2.797(1)	2.8165(9)	2.697(4)
O12	2.816(3)	2.810(1)	2.7906(9)	2.672(4)
Mean (VII)	2.384	2.384	2.404	2.438

	Nambulite	Nambulite	Natronambulite		Marsturite
	Fianel, Switzerland	Gozaisho, Japan	M5(Na)-Oi	M5(Li)-Oi	Molinello, Italy
M5- O1	1.989(8)	2.121(4)	2.344(1)	2.27(2)	2.409(5)
O3	2.154(7)	2.069(3)	2.134(2)	2.19(1)	2.202(5)
O11	2.288(7)	2.345(4)	2.316(1)	2.62(1)	2.390(5)
O14	2.049(6)	1.991(4)	2.202(1)	2.02(1)	2.253(4)
O15	2.242(6)	2.255(4)	2.496(1)	2.13(1)	2.555(5)
Mean (V)	2.144	2.156		2.25	
O15'	2.712(6)	2.843(4)	2.779(1)		2.766(5)
O12	3.064(7)	3.088(5)	2.840(1)		2.837(4)
O6	3.161(6)	3.034(5)	2.710(2)		2.649(5)
Mean (VIII)	2.457	2.468	2.478		2.508

	Nambulite	Nambulite	Natronambulite	Marsturite
	Fianel, Switzerland	Gozaisho, Japan	Gozaisho, Japan	Molinello, Italy
Si1- O1	1.616(3)	1.612(1)	1.689(1)	1.635(4)
O2	1.618(2)	1.614(1)	1.6070(9)	1.611(4)
O3	1.634(2)	1.630(1)	1.619(1)	1.615(4)
O15	1.643(3)	1.647(1)	1.646(1)	1.652(4)
Mean (IV)	1.628	1.626	1.622	1.628
Si2- O3	1.641(2)	1.642(1)	1.634(1)	1.638(4)
O4	1.616(2)	1.615(1)	1.612(1)	1.608(4)
O5	1.592(2)	1.593(1)	1.590(1)	1.588(4)
O6	1.654(3)	1.652(1)	1.659(1)	1.678(4)
Mean (IV)	1.626	1.626	1.624	1.628
Si3- O6	1.640(3)	1.642(1)	1.646(1)	1.645(4)
O7	1.598(3)	1.596(1)	1.597(1)	1.586(4)
O8	1.612(2)	1.611(1)	1.608(1)	1.604(4)
O9	1.638(2)	1.644(1)	1.643(1)	1.656(4)
Mean (IV)	1.622	1.623	1.624	1.623
Si4- O9	1.617(3)	1.615(1)	1.625(1)	1.649(4)
O10	1.612(2)	1.613(1)	1.6153(9)	1.610(4)
O11	1.619(2)	1.619(1)	1.610(1)	1.601(4)
O12	1.648(3)	1.642(1)	1.668(1)	1.673(4)
Mean (IV)	1.624	1.622	1.626	1.633
Si5- O12	1.652(3)	1.655(1)	1.668(1)	1.672(4)
O13	1.594(3)	1.593(1)	1.5969(9)	1.609(4)
O14	1.624(2)	1.618(1)	1.613(1)	1.615(4)
O15	1.658(2)	1.648(1)	1.659(1)	1.668(4)
Mean (IV)	1.632	1.629	1.634	1.642
O11...O1	2.460(3)	2.459(2)	2.471(1)	2.472(6)

TABLE 8. T-O-T angles (°) of nambulite, natronambulite and marsturite

Mineral	Locality/Reference	Si1-O3-Si2	Si2-O6-Si3	Si3-O9-Si4	Si4-O12-Si5	Si5-O15-Si1
This study						
Nambulite	Fianel mine	138.5(2)	140.6(2)	142.7(2)	132.1(2)	134.7(2)
Nambulite	Gozaisho mine	138.1(1)	140.6(1)	142.4(2)	132.0(1)	135.1(1)
Natronambulite	Gozaisho mine	142.5(1)	140.1(1)	142.2(1)	131.8(1)	133.8(1)
Marsturite	Molinello mine	142.9(3)	139.7(3)	140.8(3)	132.0(3)	132.6(3)
Nambulite	Narita et al. (1975)*	144.2(3)	139.9(3)	141.2(3)	131.4(3)	133.8(3)
Nambulite	Murakami et al. (1977)*	138.2(3)	140.2(3)	142.3(3)	131.9(3)	135.1(3)
Lithiomarsturite	Yang et al. (2011)*	138.4(2)	141.2(1)	139.1(2)	133.1(1)	134.6(1)

* T-O-T angles and associated error values were calculated from published coordinates.

TABLE 9. Bond-valence sum calculations of the nambulite, natronambulite and marsturite samples

	Nambulite		Natronambulite*		Marsturite	Na-rich Nambulite	Nambulite
	Fianel mine	Gozaisho mine	Gozaisho mine		Molinello mine	Narita et al. (1975)	Murakami et al. (1977)
M1	1.96	1.97	1.93	1.93	1.91	1.88	1.94
M2	1.87	1.88	1.72	1.85	1.89	1.80	1.86
M3	2.04	2.06	2.02	2.02	2.00	2.06	2.08
M4	1.91	1.86	1.90	1.90	1.94	1.81	1.79
M5 Li-dominant	1.08(V)	0.97(V)		0.69(V)		0.84(V)	0.88(V)
M5 Na-dominant			1.60(VIII)		1.33(VIII)		
Si1	4.14	4.16	4.20	4.20	4.13	4.14	4.14
Si2	4.17	4.17	4.19	4.19	4.15	4.17	4.17
Si3	4.20	4.19	4.19	4.19	4.21	4.20	4.20
Si4	4.18	4.20	4.16	4.16	4.08	4.18	4.18
Si5	4.10	4.14	4.08	4.08	4.00	4.10	4.10
O1	1.76	1.66	1.66	1.54	1.55	1.57	1.64
O2	1.89	1.91	1.79	1.92	1.92	1.88	1.90
O3	2.21	2.25	2.49	2.22	2.39	2.25	2.23
O4	2.02	2.02	2.03	2.03	2.03	2.01	2.00
O5	1.98	1.96	1.96	1.96	1.92	1.94	1.94
O6	2.09	2.09	2.15	2.07	2.18	2.08	2.11
O7	2.00	1.99	1.98	1.98	1.98	1.98	1.97
O8	2.02	2.01	2.03	2.03	2.06	1.98	1.99
O9	2.14	2.13	2.10	2.10	2.06	2.13	2.13
O10	2.01	2.01	1.99	1.99	2.00	2.00	2.01
O11	1.55	1.52	1.69	1.48	1.65	1.56	1.51
O12	1.99	2.01	2.03	1.97	2.02	2.02	2.01
O13	1.89	1.90	1.84	1.84	1.77	1.84	1.87
O14	1.95	2.00	2.08	1.96	2.03	1.91	1.93
O15	2.11	2.10	2.16	2.10	2.09	2.04	2.08

* Because the positions of Li and Na at M5 were refined separately in natronambulite, bond-valence sums were calculated based on Li-Oi and Na-Oi distances at M5. The positions of the O atoms coordinated by the cation at M5 are considered to be influenced by the split M5 positions.

TABLE 10. The off-center shift of the cation at M5

Mineral	Locality/Reference	Li content at M5	Off-center shift (Å)	Calculated position of center of gravity		
				x	y	z
This study						
Nambulite	Fianel mine	0.72	0.647	0.3169	0.8583	0.5521
Nambulite	Gozaisho mine	0.82	0.684	0.3168	0.8580	0.5525
Natronambulite	Gozaisho mine	0.18	ave. 0.675	0.3158	0.8585	0.5545
	Off-center shift from Na and Li is 0.508 and 0.840 Å, respectively.					
Marsturite	Molinello mine	0.07	0.506	0.3160	0.8583	0.5554
Na-rich Nambulite	Narita et al. (1975)	0.50	0.525	0.3165	0.8585	0.5539
Nambulite	Murakami et al. (1977)	0.92	0.665	0.3110	0.8581	0.5524
Lithiomarsturite	Yang et al. (2011)	1	0.800	0.3153	0.8549	0.5512